

## RESEARCH SUMMARY

The western spruce budworm is an important pest of several conifers in western North American forests. A model called the Budworm Dynamics Model has been constructed that represents the population dynamics and feeding. This model is linked to the Prognosis Model, an individual tree, distant-independent stand growth model widely used in western North America.

In this paper, a foliage dynamics model is presented that translates the tree attributes carried in the Prognosis Model into foliage biomass that serves as a substrate for budworms. A tree damage model is presented that translates budworm-caused defoliation into estimates of reduced tree growth, increased mortality, and topkilling.

The component model forms and logic, sources of data and submodels, illustrations of model behavior, and a discussion of research needs are presented. This paper is a companion to one titled "The Western Spruce Budworm Model: Structure and Content", by Sheehan and others (1989).

## ACKNOWLEDGMENTS

I am grateful for the comments and insights offered by participants in the Canada/United States Spruce Budworms Program (West): Rene Alfaro, Alan Thomson, and Alan Van Sickle from the Pacific Forestry Centre, Victoria, BC; Clinton Carlson, J. J. Colbert, Dennis Ferguson, Katharine A. Sheehan, and Albert Stage, from the Forest Service, U.S. Department of Agriculture; Peter Mika from the University of Idaho; and Tom Nichols, formally a graduate student at the University of Washington, Seattle. Bruce Hostetler and Tommy Gregg provided data for examples and insights into topkilling.

Funds for this work were provided by the Canada/United States Spruce Budworms Program (West), the Intermountain Research Station, and Forest Pest

Management, The Methods Application Group, Forest Service, U.S. Department of Agriculture.

## AUTHOR

NICHOLAS L. CROOKSTON, operations research analyst, is a member of the Quantitative Analysis for Forest Management Planning and Control Research Work Unit located at the Intermountain Research Station's Forestry Sciences Laboratory, Moscow, ID.

## CONTENTS

	Page
Introduction .....	1
Design Criteria .....	2
Display Sensitivity to Management Activities .....	2
Represent All Important Host Species .....	2
Estimate Foliage Cohorts on Crown Thirds by Tree Size .....	2
Include the Prognosis Model for Stand Development .....	3
Model Overview .....	3
The Foliage Model .....	6
Total Foliage Biomass per Tree .....	6
Dividing Foliage Into Crown Thirds .....	6
Dividing Foliage Into Age Classes .....	8
Computing Initial Biomass .....	9
Biomass Before and After Feeding .....	11
Annual Foliage Dynamics .....	11
Foliage Model Behavior .....	14
The Tree Damage Model .....	18
Using the Beta Distribution .....	19
Topkill .....	22
Height Growth .....	25
Diameter Growth .....	28
Mortality .....	28
Damage Model Behavior .....	32
Conclusions and Research Needs .....	37
References .....	38

# Foliage Dynamics and Tree Damage Components of the Western Spruce Budworm Modeling System

Nicholas L. Crookston

## INTRODUCTION

The Western Spruce Budworm Modeling System is a linked set of models that represent forest stand growth and western spruce budworm (*Choristoneura occidentalis* Freeman) population dynamics. The interactions between the trees and budworms are explicitly represented in the system. The Prognosis Model for Stand Development (Stage 1973; Wykoff and others 1982) is a major component of the system. Its tasks include predicting the growth, mortality, and establishment of trees in a stand under budworm-free conditions for one or more rotations of trees. A Budworm Dynamics Model (Crookston and others 1990; Sheehan and others 1989) simulates budworm population dynamics through a short period, usually 10 years. The Budworm Dynamics Model represents all life stages of the insect, accounts for several causes of budworm mortality, simulates adult dispersal, and computes the amount of foliage consumed by larvae.

The state variables that represent stands in the Prognosis Model are not the same as those used by the Budworm Dynamics Model. For example, the Prognosis Model does not normally compute the amount of foliage biomass on each sample tree it represents. This information is needed by the Budworm Dynamics Model. Furthermore, the Prognosis Model normally does not represent budworm-caused damage in its predictions of tree growth. This step is necessary to represent the interactions between budworm and forest dynamics.

This paper describes model components that predict the amount of foliage available for budworms to eat and those that predict the impact budworm-caused damage has on tree growth, mortality, topkill, and regeneration success. It is a companion paper to Sheehan and others (1989) who described the structure and content of the Budworm Dynamics Model. A description such as this one is an abstract of the actual model. The source computer code is the only complete statement of the model (see inside back cover for information on acquiring Budworm Model programs).

A certain amount of background information is necessary to understand this paper. Consult Wykoff and others (1982) for information on the Prognosis Model. For background on the Budworm Modeling System, consult Sheehan and others (1989), Crookston and others (1990), and Crookston (1991).

The design criteria that influenced the development of this model are reviewed in the following section. The foliage dynamics model follows, along with available references to the ideas it contains and the scant data on which it is based. The behavior of the model is presented without comparing

it to actual data. Next are the models that translate defoliation into tree damage, followed by illustrations of these models' behaviors.

Some of the model components are based on little hard evidence. Future research needs are presented that summarize important gaps in our knowledge.

A comment about the measurement systems used in this paper is in order. The Prognosis Model reports output data in English units of acres, feet, inches, and so on. The Budworm Dynamics Model is a product of a joint effort between the United States and Canada and the units of measurement are all metric. The result is that both measurement systems are used in the combined model. In this paper, the units reported are those program users are likely to see in output reports. Conversions between measurement systems are provided.

## DESIGN CRITERIA

### Display Sensitivity to Management Activities

The Budworm Model was designed to forecast budworm dynamics, tree damage, and subsequent stand growth and development. Forest cultural activities can be done that mitigate losses due to budworm. The models are used to simulate the results of management actions, and the simulation results are used to evaluate the benefits of the management actions. Therefore, one design criterion for the foliage models is that they may be made sensitive to the consequences of forest management practices.

### Represent All Important Host Species

Table 1 contains a list of species represented by the Budworm Modeling System. Host species represented by the model are indicated in the table. The nonhost species are listed because estimates of total foliage biomass of nonhost also are required to represent some aspects of budworm dynamics.

### Estimate Foliage Cohorts on Crown Thirds by Tree Size

Budworm feeding and growth rates depend partly on the age-class of foliage being consumed. The amount of new foliage, 1-year-old, 2-year-old, and remaining foliage needs to be known to the Budworm Model. Three tree-size classes for each host species are used to represent a forest stand (table 2). The crown of each tree class is divided into thirds.

Table 1—Species represented by the Budworm Modeling System

Common name	Host status	Abbreviation	Scientific name
Douglas-fir	Host	DF	<i>Pseudotsuga menziesii</i> (Mirb.) Franco
Engelmann spruce	Host	ES	<i>Picea engelmannii</i> Parry
grand fir	Host	GF	<i>Abies grandis</i> (Dougl.) Lindl.
lodgepole pine	Nonhost	LP	<i>Pinus contorta</i> Dougl.
ponderosa pine	Nonhost	PP	<i>Pinus ponderosa</i> Laws.
subalpine fir	Host	AF	<i>Abies lasiocarpa</i> (Hook.) Nutt.
western hemlock	Nonhost	WH	<i>Tsuga heterophylla</i> (Raf.) Sarg.
western larch	Nonhost	WL	<i>Larix occidentalis</i> Nutt.
western redcedar	Nonhost	WC	<i>Thuja plicata</i> Donn.
western white pine	Nonhost	WP	<i>Pinus monticola</i> Dougl.
white fir <sup>1</sup>	Host	WF	<i>Abies concolor</i> (Gord. & Glend.) Lindl.

<sup>1</sup>White fir is not represented by the Inland Empire Variant of the Prognosis Model. The Budworm Model may be linked to other geographic variants of the Prognosis Model and they may represent this species.

**Table 2—Foliage cell (crown third) codes used by the Budworm Modeling System**

Tree height size class <sup>1</sup>	Tree class name	Crown third name	Foliage cell numeric code
0-7 m	small	top	1
		middle	2
		bottom	3
7-14 m	medium	top	4
		middle	5
		bottom	6
Over 14 m	large	top	7
		middle	8
		bottom	9

<sup>1</sup>7 m = 23 ft, 14 m = 46 ft.

## Include the Prognosis Model for Stand Development

The Prognosis Model—and thus the state variables it contains, its logical flow, and program architecture—was chosen as a component of the Budworm Modeling System regardless of any negative consequences that decision may have had on the development of other Budworm Model components. The overwhelming success, flexibility, and user base of the Prognosis Model made it an extremely attractive cornerstone on which to build. This context for the foliage and damage models influenced their development in the following ways:

1. To predict growth, the Prognosis Model typically uses forward difference equations, most of which were calibrated on 10-year-long increment data. The Budworm Model uses 1-year-long increments that contain even shorter increments when some budworm development stages are simulated. The structure of the foliage model needs to allow periodic (10-year) updating of tree and foliage profiles while allowing annual updating of the foliage as it is influenced by defoliation. The structure of the damage models must allow for consistent periodic updating of the Prognosis Model sample trees, even though the components of the damage model were calibrated for specific periods that differ from the Prognosis Model and from each other.

2. The Budworm Model operates on three strictly defined tree-size classes, and the Prognosis Model operates on a sample-based set of individual trees. Because the Budworm Model estimates defoliation on tree classes, a component of the damage model is required to disaggregate class-average defoliation estimates onto the individual trees that make up the classes.

## MODEL OVERVIEW

The Prognosis Model is a distance-independent individual tree model. A user enters a sample-based list of tree measurements, data describing the site conditions, and program control commands. The Prognosis Model reads the initial data, computes some calibration statistics, and prepares to enter into a growth prediction loop. This loop contains the calculations for predicting the change for trees in the inventory list, for a given growth cycle. The cycle length is usually 10 years but can be changed by the user. Within this loop, or cycle, the following steps are followed: First, any tree

harvesting that is desired by the user is simulated. Second, the normal growth rates on trees are predicted for the period of the cycle, usually 10 years. Third, the normal mortality is estimated. At this point, normal estimates of growth and mortality are known by the model. If a budworm outbreak is being simulated, the Budworm Dynamics Model is called.

The calling sequence for the Budworm Model includes three major steps. First, the foliage biomass on individual trees is estimated. The program classifies these data into three tree-size classes for each host species. These tree classes are called Budworm Model trees to distinguish them from Prognosis Model sample trees. The foliage is further classified into three crown thirds: top, middle, and bottom. The three tree-size classes and three crown thirds per tree define nine foliage cells (table 2). The foliage in each cell is divided into four foliage age classes (also known as foliage cohorts): new, 1 year old, 2 years old, and remaining.

The second step includes the Budworm Model's loops. The Budworm Model uses 1-year-long time steps; because there are 10 years in a typical Prognosis Model growth cycle, there are usually ten, 1-year-long Budworm Model cycles within a Prognosis Model cycle. During each year, the model predicts feeding done by budworms. The feeding reduces the amount of new foliage and, sometimes, older foliage as well. The foliage dynamics model ages the new foliage into 1-year-old foliage, and the 2-year-old foliage is added to the remaining foliage. A foliage death model predicts how much of the remaining foliage dies each year. A foliage birth model predicts how much new foliage is produced the following year. The process of foliage birth, feeding by budworm, aging, and natural death is simulated for each year of the 10 Budworm Model cycles.

The third step of the Budworm Model is to translate the budworm-caused damage done to the Budworm Model trees into estimates of reduced growth, increased mortality, and topkilling of the Prognosis Model sample trees.

At this point, the Budworm Model logic ends and the Prognosis Model picks up where it left off. Other than the fact that tree growth and mortality rates have been changed, and some trees have been topkilled, the Prognosis Model is unaware that the Budworm Model was involved. The fourth step of the Prognosis Model is to add increments of growth; diameter growth is added to diameter and height growth to height. Changes in crown ratio are also computed. The Prognosis Model stores the number of trees per acre represented by each sample tree; mortality is subtracted from this value. The fifth step is to summarize stand values and write reports. The process is repeated for each cycle in a Prognosis Model run.

Sheehan and others (1989) provide another summary of the linked submodels and provide figures illustrating the Budworm Modeling System organization. The description in this paper is a little different than the description found in Sheehan and others (1989) because this description emphasizes the role of the foliage and damage models. Crookston and others (1990, p. 3) provide an organizational chart of the Budworm Modeling System components that provides more data on the spatial and temporal scope of model components and their relationships to each other.

In the following presentation, several variable names are introduced. Table 3 provides a summary of the variables, subscripts, and notation used in this paper.

**Table 3**—Variables, subscripts, and notation used in this paper

Variable or notation	Description
$\Sigma_n$	Summation over all $n$ elements
$a$	Foliage age class subscript, 1 = new, 2 = 1-year-old, 3 = 2-year-old, and 4 = remaining
$AGE_{hcat}$	The amount of biomass that will be aged from a younger age class to an older one
$APB_{hcat}$	Adjusted potential biomass
$BAF_{hcat}$	Biomass after feeding
$BBF_{hcat}$	Biomass before feeding
$BIO_n$	Prognosis Model sample tree biomass computed from Moëur (1981)
$c$	Crown foliage cell subscript defined in table 2
$CL_n$	Crown length in feet
$CMD_n$	Cumulative (5-year) defoliation
$CR_n$	Crown ratio
$D_n$	Diameter at breast height in inches
$DDS_n$	Periodic (10 years) growth in squared diameter (inches)
$DEF_n$	Defoliation proportion; the exact computation depends on the use of this variable
$f1_c$	The function illustrated in figure 1
$f2_i$	A function that predicts proportion defoliation by host, crown cell, and foliage age class; this function represents the Budworm Dynamics Model
$f3$	The function illustrated in figure 2
$h$	Host subscript
$H_n$	Height in feet
$HG_n$	Height growth in feet
$n$	Prognosis Model sample tree subscript
$s$	Tree-size class subscript, 1 = small, 2 = medium, and 3 = large
$S(c)$	An indexing function that returns tree size 1 for crown cells 1, 2, or 3; tree size 2 for crown cells 4, 5, or 6; and tree size 3 for crown cells 7, 8, and 9
$t$	Time subscript, where 1 = Initial (Inventory) year within a Prognosis Model cycle. $t$ usually runs from 1 to 10
$T$	The number of years the model has run thus far. For example, if the model is in the fourth year of a run, $T = 4$ and if the model is in the tenth year $T = 10$
$TPA$	Stand density in trees per acre
$PB_{hcat}$	Potential biomass by host, crown cell, and age
$PEDDS_{hst}$	Proportion of expected basal area increment by host and tree size
$PEHG_{hst}$	Proportion of expected height growth by host and tree size
$PRB_{hcat}$	Proportion retained biomass by host, crown cell, and age
$PRK_n$	Proportion of stem killed
$PROB_n$	The number of trees per acre represented by Prognosis Model sample tree $n$
$PTK_n$	Probability of topkill
$PMRT_n$	Probability of tree mortality
$WT_{hs}$	The number of Budworm Model trees per unit area

## THE FOLIAGE MODEL

### Total Foliage Biomass per Tree

The amount of total biomass on each Prognosis Model sample tree is estimated using models developed by Moeur (1981). She published several models that predict total foliage biomass for undamaged trees using variables carried in the Prognosis Model. One of the models was chosen to use here:

When  $D_n$  (d.b.h. inches)  $< 3.5$

$$BIO'_n = \exp (B0_n + 1.468 \ln D_n + 0.3088 \ln DDS_n - 1.077 \ln H_n + 0.6908 \ln CL_n - 0.1421 \ln TPA + 0.3992 \ln RD_n) \quad (1)$$

otherwise

$$BIO'_n = \exp (B1_n + B2_n \ln CL_n - 0.12975 \ln TPA + 0.4035 \ln H_n) - 1.13178 \quad (2)$$

where

$BIO'_n$  = biomass in pounds per tree for tree  $n$

$B0_n, B1_n$ , and  $B2_n$  = species-specific constants for tree  $n$  (see table 4)

$D_n$  = diameter at breast height (d.b.h.) in inches of tree  $n$

$DDS_n$  = periodic (10-year) increment in the square of d.b.h. for tree  $n$  (proportional to basal area increment)

$H_n$  = height in feet of tree  $n$

$CL_n$  = crown length in feet of tree  $n$

$TPA$  = stand density in trees per acre

$RD_n$  = d.b.h. of tree  $n$ , divided by quadratic mean stand d.b.h.

Then pounds are converted to grams:  $BIO_n = 453.6 BIO'_n$ .

### Dividing Foliage Into Crown Thirds

**Available Data**—Jenson (1976) studied the foliage distribution within one codominant Douglas-fir tree in the Cascade Mountains of Washington. Table 5 presents the foliage weight for that tree by whorl and foliage age class.

The whorls of Jenson's tree were arbitrarily divided into three groups—each group corresponding to a crown third. For small trees, whorls 1 to 3

Table 4—Species-dependent coefficients for the total foliage biomass equations (from tables 9 and 13 of Moeur 1981)

Species <sup>1</sup>	Intercepts		ln CL
	$D_n \geq 3.5$ B0	$D_n < 3.5$ B1	$D_n < 3.5$ B2
WP	2.66607	-1.94951	1.22023
WC	3.05935	-2.24876	1.37600
WL	1.75654	-4.73762	1.98479
WH	2.65457	-4.17456	2.00749
AF	3.06017	-1.60998	1.32649
LP <sup>2</sup>	2.622505	-3.13488	1.62368
GF	3.11508	-2.43200	1.60270
ES	3.30085	-2.93508	1.96125
DF	2.70587	-2.93508	1.25837
PP	2.45249	-2.74410	1.58171

<sup>1</sup>See table 1 for species list.

<sup>2</sup>B0 for LP is a coefficient fit for whitebark pine (*Pinus albicaulis* Engelm.).

**Table 5**—Foliage biomass by whorl and four age classes for one codominant Douglas-fir tree from the Washington Cascade Mountains (reorganized<sup>1</sup> data from table 9 of Jenson 1976)

Whorl	Foliage age class								Total
	New		1-yr-old		2-yr-old		Remaining		
	Pct	<sup>2</sup> g	Pct	g	Pct	g	Pct	g	
1	100	1	0	0	0	0	0	0	1
2	85	11	15	2	0	0	0	0	13
3	67	28	28	12	5	2	0	0	42
4	54	24	38	19	8	4	0	0	49
5	41	36	34	30	18	16	7	6	89
6	39	43	32	35	19	21	10	11	109
7	34	60	32	56	23	40	11	19	176
8	31	56	28	50	23	41	18	32	181
11	119	49	22	57	19	49	40	104	260
14	110	29	21	61	18	52	51	198	290
17	177	23	16	52	15	49	62	201	324
20	200	0	0	0	1	1	99	21	22

<sup>1</sup>Some of the percentages reported by Jenson are slightly altered so that each row sums to 100 percent.

<sup>2</sup>Grams dry weight.

represent the top third, whorls 4 to 6 represent the middle third, and whorls 7, 8, and 11 represent the bottom third. This represents an 11-year-old tree, which is a reasonable assumption for an average tree between 0 and 7 m tall. For medium and large trees, whorls are assigned to thirds as follows: top third is whorls 1 to 5, middle third is whorls 6 to 11, and bottom third is whorls 14 to 20. Table 6 illustrates the percentages of the total foliage in each crown third of Jenson's tree using these arbitrary whorl classifications.

Schmid and Morton (1981) reported mean percentage foliage area and biomass in various crown levels of Douglas-fir and white fir. They sampled eight open-grown Douglas-fir and 10 white fir from Capulin Mesa near Los Alamos, NM. Carolin and Coulter (1972) list percentages of foliage area for crown thirds of Douglas-fir trees sampled in Oregon. All these data, including the data from table 6, are displayed in table 7.

**Using a Volume Approach**—Another method for computing the percentages of total foliage by thirds is to classify a tree into a crown shape, compute the volume of each third, and express the volume as a percentage of the total. It is useful to compare the percentages presented in table 7 to those derived analytically for a given crown shape. A convenient crown shape for this comparison comprises of a cylinder of radius  $r$  and height  $2h$  for the bottom two-thirds, and a cone of radius  $r$  and height  $h$  for the top third. The crown length of our hypothetical tree is  $3h$ . Using this method, the crown volume in the top is approximately 14 percent, for the middle and bottom thirds it is 43 percent.

**Technique Used**—There is a notably strong similarity between all of the estimates for medium to large Douglas-fir trees. The similarity between percentage of foliage area and percentage foliage weight is strong in Schmid and Morton's (1981) data. This lends support to the idea that measurements of percentage foliage area by Carolin and Coulter (1972) can be considered as additional data. The percentages derived from Jenson's

Table 6—Biomass by crown third for Jensen's (1976) tree using arbitrary whorl classification to define crown thirds

Tree class	Crown third							
	Top		Middle		Bottom		Total	
	Pct	g	Pct	g	Pct	g	Pct	g
Small	6	56	27	245	67	617	100	918
Medium and large	12	191	47	723	41	637	100	1,151

Table 7—Summary of data on percentage of foliage by crown thirds

Description and source	Crown class		
	Top	Middle	Bottom
Small DF trees, percentage of biomass (table 6)	6	27	67
Medium and large DF trees, percentage of biomass (table 6)	12	47	41
Medium DF trees, percentage of biomass (Schmid and Morton 1981)	16	55	29
Medium DF trees, percentage of foliage area (Schmid and Morton 1981)	15	52	33
Medium WF, percentage of biomass (Schmid and Morton 1981)	24	49	27
Medium WF, percentage of foliage area (Schmid and Morton 1981)	24	44	32
Medium DF, percentage of foliage area (Carolin and Coulter 1972)	12	36	52
Volume approach described in this paper	14	43	43
Values used in the model			
Small trees	5	30	65
Medium and large trees	15	45	40

(1976) data, the volume approach, and the direct measurements are similar. The choice of arbitrary divisions in the whorl numbers of Jensen's tree yielded percentages that are not grossly different from the other measurements.

I believe that errors in estimating proportions of foliage in crown thirds are relatively unimportant to meeting the objectives of this foliage model. Therefore, I computed a simple average of the percentage data and adjusted the numbers to even 5 percentage points such that their sum equals 100 percent (see the bottom of table 7).

## Dividing Foliage Into Age Classes

Within each crown third, the percentages of the foliage that are new, 1-year-old, 2 years old, and the remaining need to be computed.

**Available Data**—Jensen's (1976) DF (see table 1 for species abbreviations) tree data (table 5) can be organized into the whorl groups used to divide the foliage into crown thirds. The relative amount of foliage by foliage age class can then be computed for the crown thirds. These data are displayed in table 8.

Table 8—Biomass by foliage age class for each crown third derived from Jenson's (1976) data, table 5

Tree size class	Whorl numbers	Crown third	Foliage age class							
			New		1-yr-old		2-yr-old		Remaining	
			Pct	g	Pct	g	Pct	g	Pct	g
Small	1-3	Upper	71	40	25	14	4	2	0	0
	4-6	Middle	42	103	34	84	17	41	7	17
	7-11	Bottom	27	165	26	163	21	130	25	155
Medium,	1-5	Upper	52	100	33	63	12	22	3	6
Large	6-11	Middle	29	208	27	198	21	151	23	166
	14-20	Bottom	8	52	18	113	16	102	58	370

Hatch and Mika (1978) reported the percentage of new foliage on 18-inch-long midcrown sample branches from DF and GF. For DF, the mean was 27 percent and the standard deviation was 13 percent. For GF, the mean was 35 percent and standard deviation was 7 percent. These data do not include an estimate of the percentage of new foliage on the crown third. The 18-inch-long samples may or may not include all needle cohorts in the midcrowns. However, the mean Douglas-fir estimate from Hatch and Mika is 27 percent, and the percentage for Jenson's tree is 29 percent. This fact supports the data derived from Jenson's tree.

No other data on foliage profiles were found for the host species.

**Technique Used**—Table 9 displays the percentages used in the foliage model to partition foliage in each crown third. These values are not identical to those in table 8; they are slightly different due to arbitrary rounding to ensure the two totals sum to 100 percent and, in the case of upper crowns, a small amount of remaining foliage is present. The reason the remaining foliage was added to the upper crowns of small trees is related to computational convenience within the dynamic part of the foliage model (described below).

## Computing Initial Biomass

**Potential Biomass**—Recall that Moeur's (1981) models (equations 1 and 2) estimate total foliage biomass on an undamaged tree, and that those estimates are converted to grams in variable  $BIO_n$ . Let  $PB_{hca}$  be the total biomass per tree for host  $h$ , foliage cell  $c$  (see the nine foliage cell codes defined in table 2), and foliage age class  $a$  (1 = new, 2 = 1-year-old, 3 = 2-year-old, and 4 = remaining foliage). Then:

$$PB_{hca} = \sum_n (BIO_n PA_{ca} PC_c PROB_n) / \sum_n PROB_n \quad (3)$$

where

$\sum_n$  = denotes a summation over sample trees of host  $h$

$PA_{ca}$  = proportion of foliage of age class  $a$  within foliage cell  $c$  (see table 9)

$PC_c$  = proportion of the tree biomass in crown class  $c$  (see table 7)

$PROB_n$  = trees per acre represented by tree  $n$ .

**Adjusted Potential Biomass**—In a budworm-infested forest, the actual biomass differs from potential biomass because budworm feeding alters the tree's foliage profile. The amount of old foliage can be greater than normal due to trees' tendency to retain old needles longer than normal during

Table 9—Percentage of new, 1-year-old, 2-year-old, and remaining foliage by crown third for undamaged trees

Tree size class	Crown thrd	Foliage age class			
		New	1-yr-old	2-yr-old	Remaining
Small	Upper	70	24	4	2
	Middle	45	30	20	5
	Bottom	35	30	25	10
Medium	Upper	50	35	12	3
	Middle	30	25	20	25
	Bottom	10	20	20	50
Large	Upper	50	30	15	5
	Middle	30	25	20	25
	Bottom	10	20	20	50

periods of defoliation. A. Van Sickle (in Thomson 1979, p. 12) reported this phenomenon.

The amount of new foliage produced by a tree is partly a function of the defoliation during the preceding year. Defoliation-caused reductions in food reserves reduce the number of needles in buds and the weight of new foliage in balsam fir (Mayfield 1984). Thomson (1979) hypothesized that the same phenomenon occurs in Douglas-fir and suggests that new foliage depends partly on defoliation of new foliage in the previous year. Thomson's suggested function was parameterized for the tree classes used in the Budworm Model (fig. 1). The parameters were chosen in 1982 to match a hypothesis proposed by some of the scientists listed in the acknowledgments of this paper.

The adjusted potential biomass before feeding ( $APB_{hcat}$ ) for time  $t = 1$  (the inventory year) is computed from  $PB_{hca}$ , the functions illustrated in figure 1, and inventory-time estimates of previous defoliation:

$$APB_{hcat} = PB_{hca} fI_c(PRB_{hc(a+1)t}) \quad (4)$$

where

$PRB_{hcat}$  = proportion retained biomass for host  $h$ , crown  $c$ , foliage age class  $a$ , at time  $t$

$h$  = host species

$c$  = foliage cell code (table 2)

$a$  = foliage age classes 1, 2, and 3

$t$  = 1 (inventory time)

$fI_c$  = function illustrated in figure 1, indexed by foliage cell.

The inventory-time estimates of the proportion of retained biomass are entered by the model user (Crookston and others 1990, p. 7). For example, a value of 0.80 for a given age class in a given crown of a given host is an indication that 20 percent of the biomass on that branch was missing (presumably eaten or destroyed by budworms). Values of  $PRB$  for the remaining foliage class may be greater than 1.0 indicating that more than normal levels of remaining biomass were present at inventory time.

The adjusted potential biomass corresponds to the amount of foliage an observer would measure on a tree that may have been defoliated in the recent past but is not currently defoliated. Within the Budworm Model,  $APB$  is the denominator used to compute percentage defoliation.

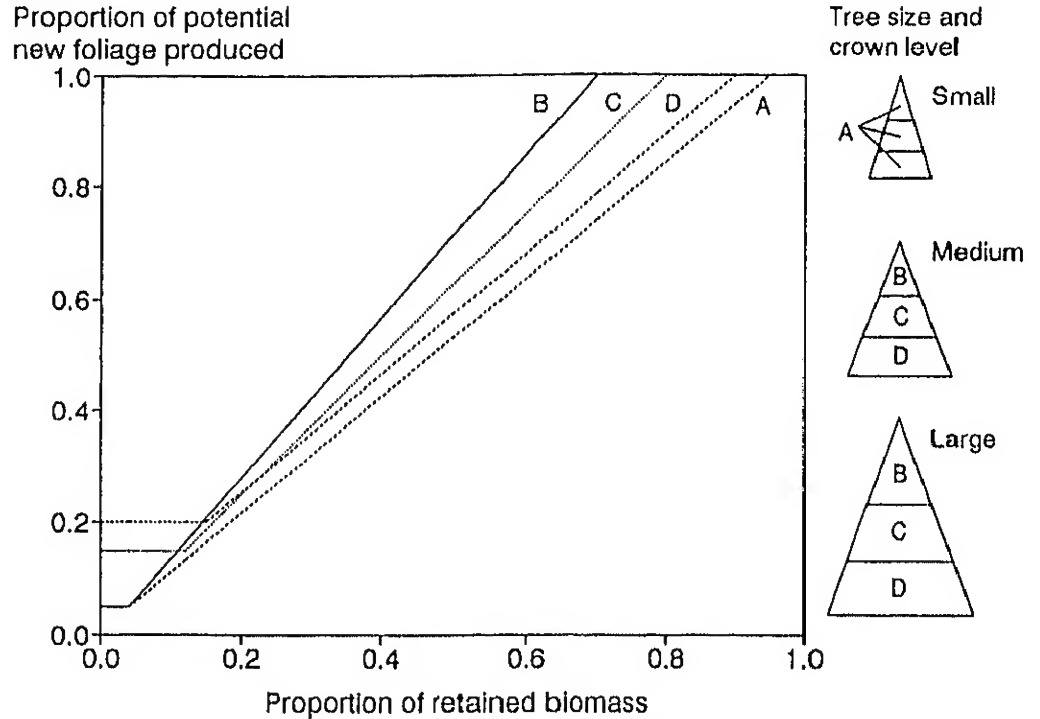


**Figure 1**—Relationship between proportion of retained biomass and the proportion of the potential new foliage a tree can produce. Line A applies to all crown levels of small trees, line B applies to the tops of medium and large trees, line C applies to the middle of medium and large trees, and line D applies to the bottom of medium and large trees.

## Biomass Before and After Feeding

Biomass before feeding ( $BBF$ ) is the amount of foliage available to budworms. The initial computation of  $BBF$  is

$$BBF_{hcat} = APB_{hcat} PRB_{hcat} \quad (5)$$

for all four age classes; the other variables are as defined above. The Budworm Model contains component models that convert the new foliage class into bud numbers and simulates budworms eating buds developing new foliage. Spring foliage development rates are predicted using models developed by Beckwith and Kemp (1984). Biomass after feeding ( $BAF$ ) is represented by

$$BAF_{hcat} = BBF_{hcat} f2_{hcat} \quad (6)$$

where  $f2$  represents proportion defoliated by the Budworm Model on host  $h$ , crown  $c$ , age  $a$ , and in year  $t$ . There is an option in the Budworm Model (Crookston and others 1990, p. 7) that allows users to circumvent the Budworm Dynamics Model and directly enter values for  $f2$ . This option was used in preparing examples of behavior for this paper because it allows users to isolate the behavior of the foliage dynamics and damage components from the behavior of the Budworm Dynamics Model.

## Annual Foliage Dynamics

Foliage estimates for time  $t = 2, 3, \dots, 10$  are computed as described below.

**Recompute Proportion of Retained Foliage**—After a year of feeding, a new estimate of  $PRB$  can be computed:

$$PRB_{hcat} = BAF_{hcat} / APB_{hcat} \quad (7)$$

**Compute Remaining Foliage**—The amount of remaining foliage depends on the amount being added from the 2-year-old foliage class as this foliage ages, and the amount that dies. The idea of retaining old biomass described earlier is incorporated in this model.

**Part I:** The foliage model assumes that whatever the current status of remaining foliage, the tree tends toward normal levels when defoliation stops. When  $PRB_{hc1t}$  is greater than or equal to 0.80 (new foliage defoliation is less than 20 percent), the model assumes that defoliation of new foliage during year  $t$  has essentially stopped. The amount of remaining foliage present when defoliation stops can be greater, equal, or less than the amount found on undamaged trees. Excess old foliage (40 percent per year) dies quickly; below-normal amounts are replaced by aging 2-year-old foliage.

The aging of 2-year-old foliage into the remaining foliage age class is complicated by the differences in the potential biomass in the 2-year-old and remaining class. The proportionate difference between these classes is used to scale the amount of biomass that moves from the 2-year-old to remaining. Let  $AGE_{hc(a+1)t}$  be the amount of foliage aging from age class 3 to class 4, in host  $h$ , crown  $c$ , at time  $t$ :

$$AGE_{hc4t} = BAF_{hc3t}(PB_{hc4}/PB_{hc3}) \quad (8)$$

The rest of Part I of the remaining biomass calculations are as follows:

If  $BAF_{hc4t} \geq PB_{hc4}$  then

$$BBF_{hc4(t+1)} = PB_{hc4} \text{ when } (BAF_{hc4t} - PB_{hc4})/PB_{hc4} < 0.10, \text{ otherwise } BAF_{hc4t} - (0.4 (BAF_{hc4t} - PB_{hc4})) \quad (9)$$

If  $BAF_{hc4t} < PB_{hc4}$ , let  $X = BAF_{hc4t} + AGE_{hc4t}$  then

$$BBF_{hc4(t+1)} = X \text{ when } X < PB_{hc4} \text{ and } PB_{hc4} \text{ otherwise} \quad (10)$$

**Part II:** When  $PRB_{hc1t}$  is less than or equal to 0.80 (defoliation is over 20 percent), the amount of remaining foliage is driven by the tree's tendency to reduce foliage mortality.

Three mortality effects are hypothesized. First, if the remaining biomass is greater than or equal to the potential biomass summed over all foliage age classes, as much biomass dies each year as is added from the 2-year-old class. This means that a tree cannot retain more biomass in the remaining category that it could potentially hold over all foliage age classes. This becomes an upper bound on the remaining foliage class. Any foliage accumulating beyond this point is killed by the model.

Second, when a tree is not being defoliated, the amount of old foliage dying approximately equals the amount being added to the old (remaining) foliage class. Thus, the intrinsic mortality of the remaining foliage would be equal to the amount of 2-year-old biomass that is aging into the remaining class. In this model, the intrinsic mortality is reduced as new foliage defoliation increases (fig. 2). The rate is further adjusted to account for the fact that the amount of old foliage dying is much smaller than the amount being added to the remaining foliage class in small trees. The rates used are specific to the host species. As modeled, Douglas-fir and spruce have a stronger ability to retain old foliage when new foliage is lost than grand fir, white fir, and subalpine fir.

The third mortality effect is directly related to total tree defoliation. It accounts for the idea that a tree's ability to retain old needles is hampered

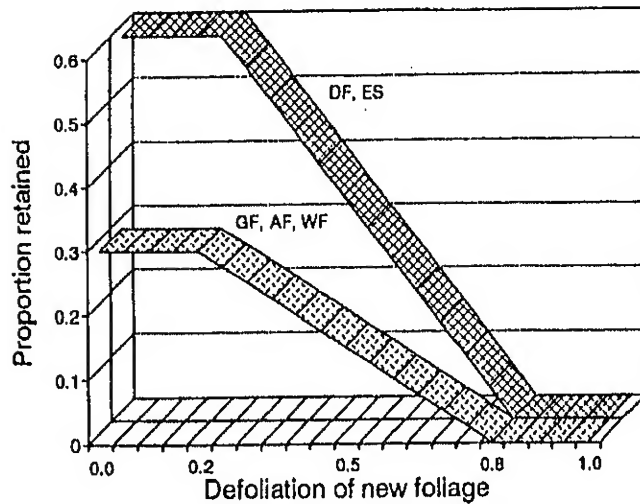


**Figure 2**—Relationship between new foliage defoliation and the proportion of the foliage entering the old foliage class that is retained. Old needle retention is stronger in Douglas-fir and spruce than in the firs.

due to branch and needle drying and sun scald coincident with opening up the canopy to additional light. Evidence that this might happen is limited to the fact that when the model was constructed without this effect, surviving heavily defoliated trees retained old needles indefinitely unless the old needles were actually eaten by budworms.

This last effect is modeled by monitoring total tree defoliation. When total defoliation exceeds 40 percent, 15 percent of the remaining foliage dies.

A formal statement of the model follows:

Let  $XM_t = 1.0$  if total tree defoliation in year  $t$  is less than 40 percent and 0.85 otherwise. Let

$$XAB_{hc4t} = (BAF_{hc4t} + AGE_{hc4t} f3(PRB_{hc1}))XM_t \quad (11)$$

where  $f3$  is the function displayed in figure 2.

Finally,

$$BBF_{hc4(t+1)} = XAB_{hc4t} \text{ when } XAB_{hc4t} < \sum_a PB_{hca}, \text{ and } \sum_a PB_{hca} \text{ otherwise.} \quad (12)$$

**Compute 1- and 2-Year-Old Foliage**—The 1- and 2-year-old foliage is computed by aging the younger foliage. The process moves the 1-year-old to the 2-year-old then the new to the 1-year-old. For  $a = 2$  and 3

$$BBF_{hca(t+1)} = BAF_{hc(a-1)t} (PB_{hca}/PB_{hc(a-1)}) \quad (13)$$

**Compute New Foliage**—The amount of new foliage each year is modeled as a function of the potential new biomass an undamaged tree can grow and the defoliation the tree has undergone. This is the same model as that used for initial conditions except that the measure of defoliation is a weighted average of two measurements. The first measurement is the retained biomass after feeding divided by biomass before feeding. The second measure of defoliation is the biomass after feeding divided by the potential biomass expected on a healthy tree.

Neither measurement has been directly related to new foliage development in field studies. However, both have some theoretical basis. The first measure is given a weight of 0.40 and the second measure a weight of 0.60. The second weight is greater than the first, implying that second measure more correctly measures the ability of the tree to regenerate foliage. The following function is used to compute new foliage in the next period:

$$BBF_{hc1(t+1)} = PB_{hc1} f1(0.4 PRB_{hc2} + 0.6 (BAF_{hc2t}/PB_{hc2})) \quad (14)$$

**Periodic Foliage Dynamics**—The annual foliage dynamics described above are used to model year-to-year dynamics for approximately 4- to 10-year-long periods. At the end of the period, the model computes a final estimate of proportion retained biomass and stores it for use at the beginning of the next period to recompute initial conditions.

The Prognosis Model estimates tree growth and mortality at every period. Therefore, at the beginning of the next period, some of the trees that were in the small- or medium-tree-size class will grow into the next class. For example, let's say your stand has a few small trees in it. The medium class is empty. At a period boundary, the trees might "move" to the next larger class. The foliage model has a provision in it that traces the movement of defoliated trees from one class to another and properly adjusts the estimates of proportion retained biomass to reflect the movement.

## Foliage Model Behavior

The behavior of this model is examined in two respects. The first concerns the changes in several state variables under different defoliation profiles. The period will be held at 10 years, and the annual behavior will be exercised, illustrated, and discussed. The second concerns the periodic behavior. In this model, the period length is user-input, and the structure of the model differs greatly on period boundaries versus annual time steps. It is important, therefore, to understand the impact changing the period length has on model behavior. The same stand and defoliation profiles are used to examine both the annual and periodic behavior.

**Description of Example Site**—The stand data used in the examples of behavior were collected from Bear Gulch, about 20 km south of John Day, OR. The site is a long and steep north-facing slope visible to travelers of U.S. Highway 395. The south-facing slope to the north of the study site contains little timber; the same is true for the south-facing slope located south of the study site. Therefore, the site is bounded on the north and south by a significant area of essentially nontimber lands. The area is a Douglas-fir site that contained many large ponderosa pine trees until they were logged in the mid-1980's. The remaining stand of mostly Douglas-fir was heavily defoliated by western spruce budworm soon after the site was logged. Table 10 lists several characteristics of the example site (this site is used in Crookston [1991] as well).

Three defoliation profiles are applied to the stand (table 11). For case 1, 95 percent defoliation of the new foliage and 40 percent of the 1-year-old foliage is applied for each year of a 10-year simulation. Case 2 is the same except that defoliation is stopped after 5 years. Case 3 uses variable defoliation, which more nearly typifies actual experience. All tree-size classes and foliage cells are treated identically.

**Indicator Variables**—Five variables are plotted over time to illustrate the behavior of the foliage dynamics models. All of the figures use the same format. The variable labels (figs. 3-6) and definitions are as follows:

**Table 10—Mensurational characteristics of the Bear Gulch study site**

Attribute <sup>1</sup>	Value
Number of trees	
per hectare	1,003
per acre	406
Basal area	
m <sup>2</sup> /ha	25.0
ft <sup>2</sup> /acre	109
Top height	
meters	23.2
feet	76.3
Merchantable volume	
m <sup>3</sup> /ha	157.9
ft <sup>3</sup> /acre	2,256
Percent Douglas-fir	89
Percent ponderosa pine	11

<sup>1</sup>Conversion factors: 1 ft = 0.3048 m,  
1 inch = 2.54 cm, 1 acre = 0.4047 ha,  
1 ft<sup>2</sup>/acre basal area = 0.2296 m<sup>2</sup>/ha,  
1 ft<sup>3</sup>/acre merchantable volume = 0.0700 m<sup>3</sup>/ha.

**Table 11—Percentage defoliation values used in the three test cases**

Year	Case 1		Case 2		Case 3	
	New	1-yr-old	New	1-yr-old	New	1-yr-old
1	95	40	95	40	0	0
2	95	40	95	40	100	10
3	95	40	95	40	20	0
4	95	40	95	40	90	20
5	95	40	95	40	20	0
6	95	40	0	0	95	10
7	95	40	0	0	50	0
8	95	40	0	0	0	0
9	95	40	0	0	0	0
10	95	40	0	0	0	0

**Adj-Pot** Adjusted potential biomass in grams per tree on an average tree prior to defoliation each year. Let  $WT_{hs}$  be the number of trees per unit of area of host  $h$  and tree size  $s$  and  $S(c)$  be a function that provides a tree size  $s$  given a crown index  $c$ . Then:

$$Adj-Pot_t = (\sum_h \sum_c \sum_a APB_{heat} WT_{hS(c)}) / \sum_h \sum_c WT_{hS(c)} \quad (15)$$

**Tot-Post** *Adj-Pot* after feeding.

**Rem-Post** Remaining biomass in grams per tree after feeding on an average tree.

$$Rem-Post_t = (\sum_h \sum_c BAF_{heat} WT_{hS(c)}) / \sum_h \sum_c WT_{hS(c)} \quad (16)$$

**New-Pre** New biomass in grams per tree before feeding on an average tree.

$$New-Pre_t = (\sum_h \sum_c BBF_{heat} WT_{hS(c)}) / \sum_h \sum_c WT_{hS(c)} \quad (17)$$

**New-Post** *New-Pre* after feeding.

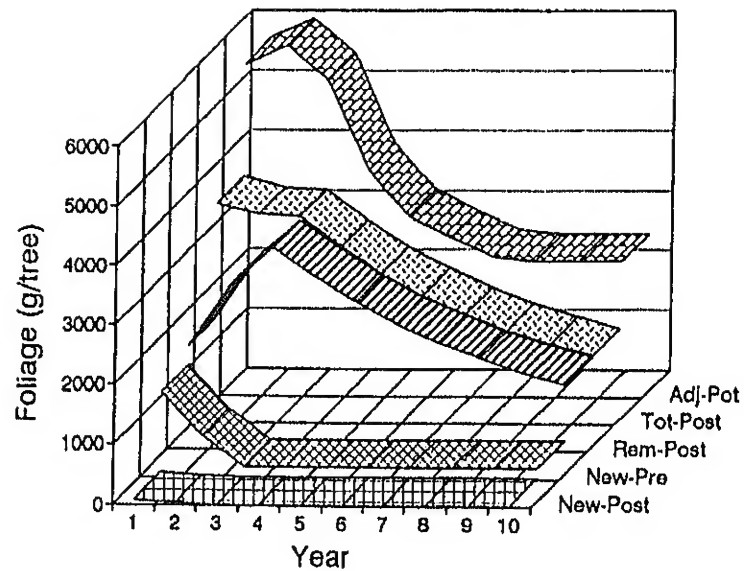


**Figure 3—Foliage dynamics for case 1 (table 11)** indicated by Adj-Pot, the adjusted potential biomass on an average tree; Tot-Post, which is Adj-Pot after defoliation; Rem-Post, the biomass of remaining foliage after defoliation; New-Pre, the new biomass before defoliation; and New-Post, the new biomass after defoliation (refer to the text for complete definitions).

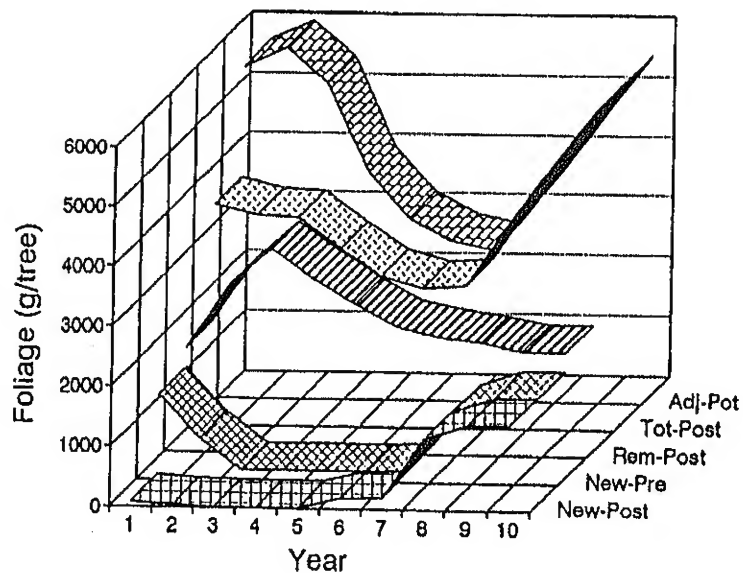


**Figure 4—Foliage dynamics for case 2 (table 11)** illustrated by plotting five indicator variables over time (see fig. 3 and text).

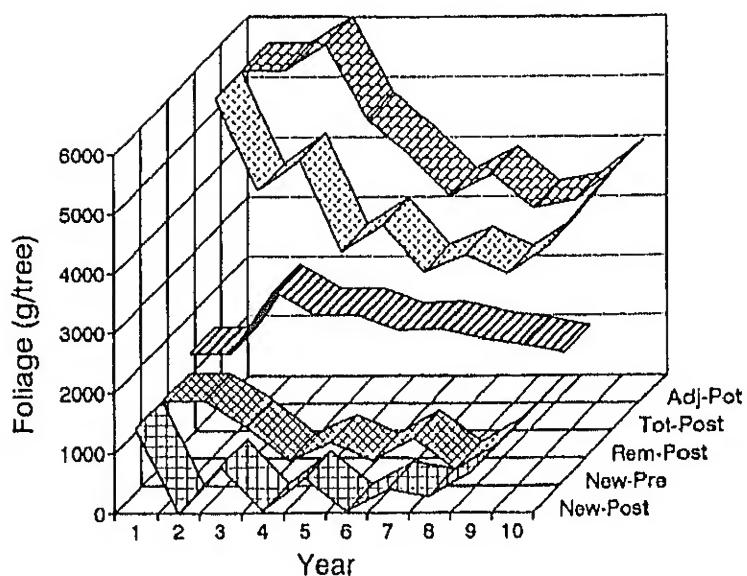


**Figure 5**—Foliage dynamics for case 3 (table 11) illustrated by plotting five indicator variables over time (see fig. 3 and text).

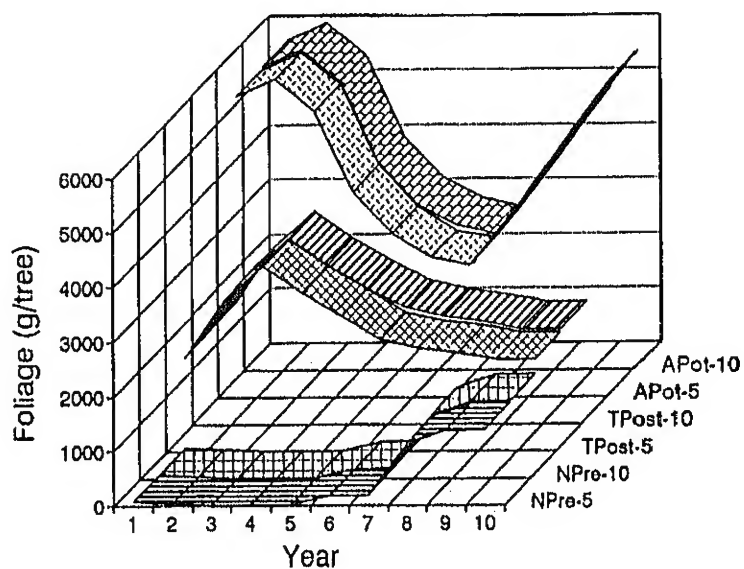


**Figure 6**—Foliage dynamics for case 2 run in one 10-year-long Prognosis Model cycle (APot-10, TPost-10, and NPre-10) and in two 5-year-long Prognosis Model cycles (APot-5, TPost-5, and NPre-5). The difference between pairs of lines is due to changes caused by the Prognosis Model cycle boundary. Label associations with those used in figures 3-5 are: APot = Adj-Pot, TPost = Tot-Post, NPre = New-Pre.

**Annual Behavior**—Annual behavior is examined by running the model for 10 years without exercising the periodic component of the model. Figure 3 corresponds to case 1 (table 11), figure 2 to case 2, and figure 4 to case 3. The initial conditions (year 1, figure 3) indicate that there are 5,200 g per tree of adjusted potential biomass, and because there had been no previous defoliation, the adjusted potential (*APB*) and the potential (*PB*) are the same. There are just over 1,000 g per tree of new foliage available for the first generation of budworms to feed on.

In case 1 (fig. 3) the adjusted potential and remaining foliage age class rises for the first year following heavy defoliation. This rise is due to the model component that increases old needle retention at the onset of defoliation. As high defoliation continues, the needles from the remaining class die, resulting in a steady decline in foliar biomass in the remaining class as well as on the entire tree. New foliage prior to defoliation is over 1,000 g in the first year then drops to below 300 g in subsequent years. This is due to the model components that represent the effect defoliation has on new foliage production.

In case 2 (fig. 4), the same trends exhibited in figure 3 are evident for the first 5 years. After the fifth year, the foliage recovery is displayed. New foliage biomass returns to preoutbreak levels in about 3 years. Foliage in the remaining class returns to preoutbreak levels quickly because the levels were not far from normal when the defoliation stopped. All of the indicators return to normal before the end of the 10-year cycle.

Case 3 (fig. 5) illustrates the interaction of the foliage model components. The pulses of defoliation caused the foliage model to respond by reducing the amount of new foliage in the next year; remaining needles were retained and the total in this foliage age class increased. All of the effects of defoliation were followed by the effects of recovery when the defoliation levels were low.

**Periodic Behavior**—All three cases were run using one 10-year-long Prognosis Model cycle and then using two 5-year-long cycles. Figure 6 displays the results of running case 2. Three of the five indicator variables are illustrated as pairs of lines in figure 6. All three are closely related, suggesting that the foliage dynamics model behaves similarly when there is a cycle boundary in the middle of an "outbreak" as compared to running one 10-year-long cycle. The other cases are not illustrated because the "cycle boundary" effect was even smaller in those cases than in case 2.

The effect of tree growth between cycles is minimal during an infestation. This is partly due to the fact that defoliated trees do not grow well. In a model run of lightly defoliated trees that are fast growing, a discontinuity in the indicator variables caused by tree growth will be more evident. Figure 6 shows a slight difference in the lines labeled TPost-5 and TPost-10 starting at year 5. This difference is due to tree growth.

The effects of a cycle boundary in the middle of a Budworm Model run are not strong as far as the foliage dynamics model is concerned. There may be other subcomponents of the Budworm Modeling System that are less well behaved in this respect.

## THE TREE DAMAGE MODEL

Defoliation of trees reduces diameter and height growth, increases mortality rates, causes topkilling, and influences the success of regeneration establishment. More is known about the effects of defoliation on tree

growth than is known about the foliage dynamics of defoliated trees. However, each study that relates the effects of defoliation on tree growth and development uses a different measurement of defoliation. Therefore, part of the damage model is devoted to computing defoliation metrics.

The Budworm Model represents trees as classes: small, medium, and large; and the Prognosis Model represents trees as individual sample trees. The defoliation predicted on a given Budworm Model tree class is considered an average for all of the Prognosis Model trees in the class. In natural stand conditions, all trees within a tree-size class do not have identical defoliation patterns (McDonald 1981). To represent this variation, the simulated average defoliation for each tree class is distributed to the Prognosis Model sample trees that make up the class following the Beta distribution. The reasons for using the Beta distribution and the way the distribution parameters are computed are described next.

## Using the Beta Distribution

**Data**—To develop growth equations for budworm-defoliated small trees, Ferguson (1988) measured the defoliation in the tops, middles, and bottoms of individual trees on each sample study site. Ferguson's data, augmented with a small portion of data taken in Oregon, were used to parameterize the Beta distribution used in the damage model. The trees on each study site were classified into the tree-size classes used by the Budworm Model (table 2). Figure 7 plots the variance of the individual tree defoliation measures over the mean for each foliage cell and study site. Cases with less than four observations were deleted.

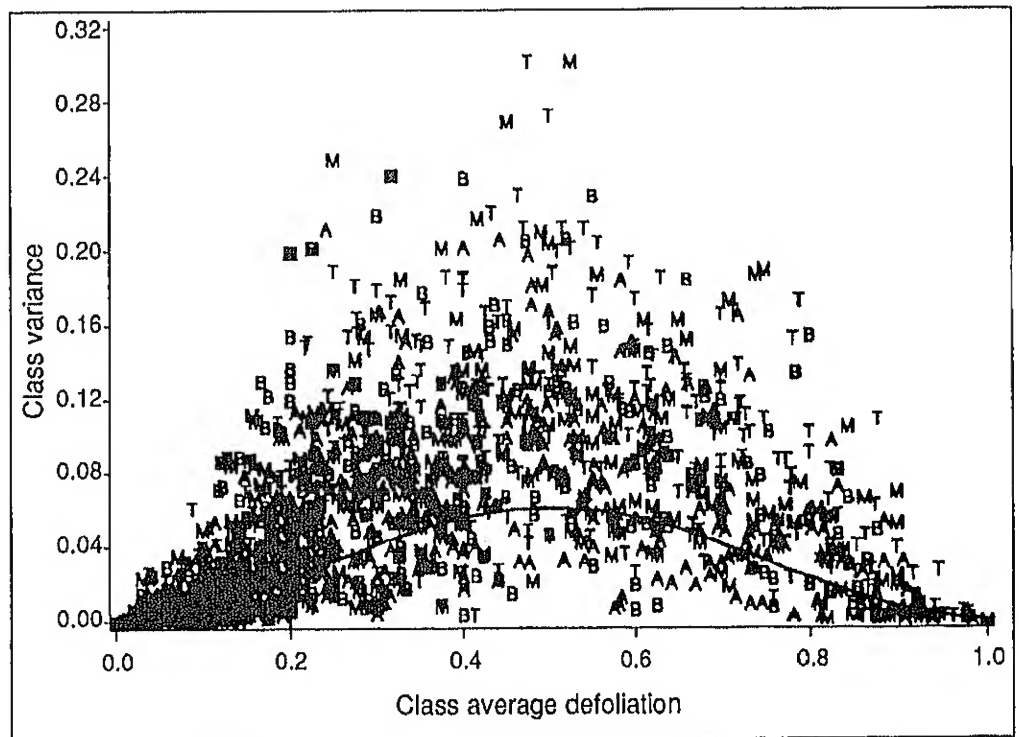


**Figure 7**—The class variance of individual tree defoliation measures plotted over the class average. Symbols are T = top crown third, M = middle third, B = bottom third, and A = average of T, M, and B. The solid line represents the function used by the model to compute a class variance given the class average.

As the mean defoliation increases toward 50 percent, the variance also increases, and when the mean exceeds 50 percent, the variance diminishes toward zero. Theoretically, the variance of proportion data must be zero when the mean is zero or 100 percent. The peak variance could be shifted to the right or left of 50 percent (the underlying distribution need not be binomial). These data indicate the peak is near 50 percent and that the distribution is not asymmetrical. (The line in fig. 7 is discussed below.)

**Justifications**—The justifications for using the Beta are as follows. First, 100 percent of the probability density function (p.d.f.) is contained on the interval (0-1). Second, the shapes of the p.d.f. are appropriate for these data. The shape parameters ( $v$  and  $w$ ) for the p.d.f. are estimated from the sample mean,  $\bar{x}$  and variance,  $s^2$  (Hastings and Peacock 1975):

$$v = \bar{x}((\bar{x}(1-\bar{x})/s^2) - 1) \quad (18)$$

$$w = (1-\bar{x})((\bar{x}(1-\bar{x})/s^2) - 1) \quad (19)$$

Figure 8 illustrates several shapes of the Beta where the mean is set to 0.5 (50 percent) and the variance is varied from 0.02 to 0.12. When the variance is low, most of the probability density is near the mean. When the variance is high, the probability density is pushed toward the tails. For defoliation data, the Beta appropriately implies that if a class of trees has a mean proportion defoliated of 0.5 (50 percent) and a variance of 0.12, then the number of trees defoliated between 0 and 0.1 (10 percent) plus those defoliated between 0.9 and 1.0 would exceed the number defoliated between 0.4 and 0.6. If the variance is 0.02, the number defoliated between 0.4 and 0.6 would exceed the number found in the tails of the distribution.

**Calculating the Parameters**—The data in figure 7 clearly indicate that the class variance is much lower when the mean is low or high than it is when the mean is 0.5. The line in figure 7 illustrates a reasonable, albeit very conservative, representation of the relationship between class variance and class mean. This function is taken from the Weibull p.d.f.:

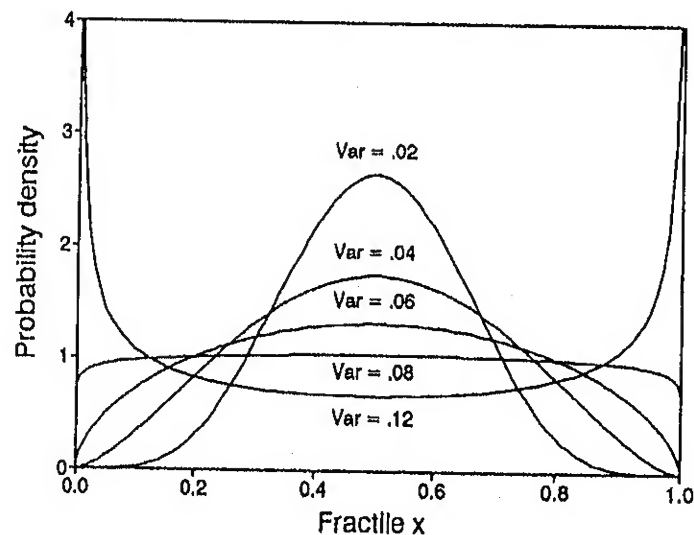


Figure 8—The Beta probability density function for several variances with the mean held constant at 0.5.

$$s^2 = a V (c \bar{x}^{c-1} \exp(-\bar{x}^c)) \quad (20)$$

where  $a = 0.9304$ ,  $c = 2.7$ ,  $V$  is the maximum variance, and  $\bar{x}$  is the sample mean. This function is illustrated for  $V = 0.06$  and  $0.03$  in figure 9 (the reason  $V = 0.03$  is displayed will become clear in following sections). Although this function is nearly symmetrical when  $c = 2.7$ ,  $1 - \bar{x}$  is used when  $\bar{x}$  is greater than  $0.5$  to guarantee symmetry.

Figure 10 illustrates shapes of the Beta for various means whereby the variance is computed as a function of the mean using equation 20 where  $V = 0.06$ .

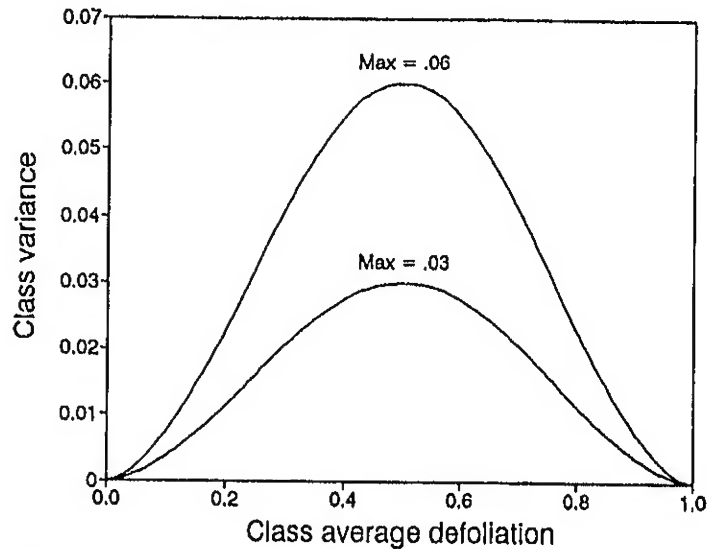


Figure 9—The class variance as a function of the class average for two values of maximum variance.

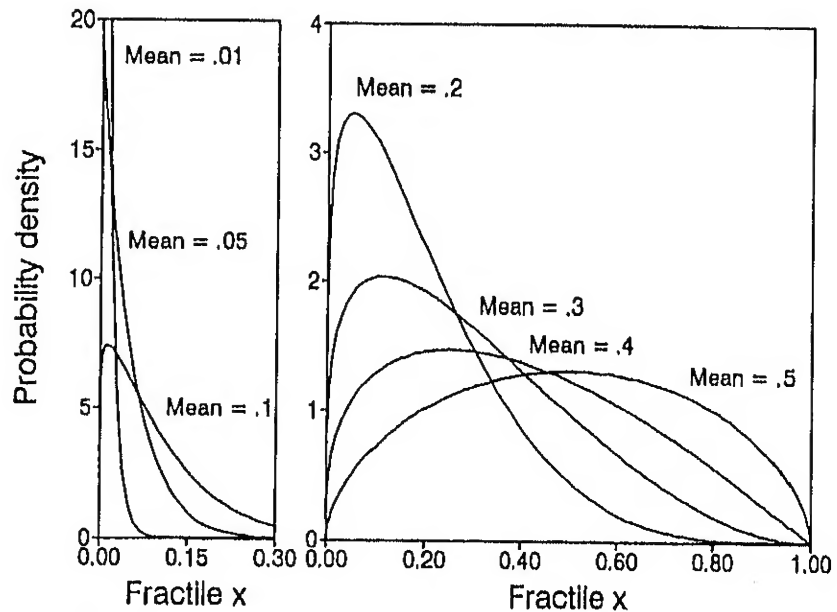


Figure 10—The Beta probability density function for several means whereby the variance is computed using the function displayed in figure 9, with maximum variance set to  $0.06$ . For means  $= 0.01$ ,  $0.05$ , and  $0.1$ , only part of the defined interval of the fractile is shown. Complementary curves exist but are not illustrated. For example, the curve for mean  $= 0.8$  is the mirror image of the one shown for mean  $= 0.2$ .

In the Budworm Modeling System, a defoliation value for an individual tree within a given tree class is generated from the Beta distribution with shape parameters derived from the relationships used to plot figure 9. Generation of Beta deviates given real shape parameters is done using the generator of Cheng (1978). In the following text, the notation

$$x = \beta(\bar{x}, V) \quad (21)$$

is used to denote that  $x$  is a Beta random variable with shape parameters computed from the mean and maximum variance (equations 18-20).

Other than described above, the Budworm Modeling System does not explicitly represent variation between individual trees. The Budworm Model trees are averages representing a range of genetic and phenologic characteristics between trees in each model class. The approach taken in the damage model represents the empirical evidence that all trees within a class are not alike with respect to defoliation. In choosing a conservative value for the maximum variance, the model is programmed to represent only a portion of the possible variance as seen in figure 7. If more information regarding the between-tree variability were available, a more complete representation of this variance may be justified.

Some of the damage models are functions of sums or averages of several years of defoliation. Ferguson's (1988) data had repeated measures, as did the data from Oregon. A similar scatter diagram to that displayed for figure 7 for the average of several years' defoliation, showed that the maximum class variance of the 4- to 5-year average is approximately half the variance of the individual year values. Therefore, a maximum variance of 0.03 is used where multiyear averages are used.

## Topkill

Topkill occurs when live tree height is reduced. The damage model represents topkilling in two phases. First, the probability of topkilling is computed. This probability is compared to a uniform random number (0, 1), and if the probability of topkill is greater than the random number, the tree is topkilled. Second, the amount of topkill is computed. The models used in this two-step process are independently derived and applied. The final component of the topkill logic concerns determining if topkilling permanently damages a tree. That is, the model assumes that trees with tops killed down to a 4-inch diameter will never produce merchantable volume above the point of topkill. If the diameter is less than 4 inches, the tree may recover a merchantable top.

**Small Trees**—Ferguson (1988, p. 6) published a "dieback" model for small trees. The probability of topkill model (fig. 11) is a function of defoliation, tree height, and crown ratio. His published model includes two defoliation terms with unequal constants. In the Budworm Model, these terms are combined to produce the following:

$$PTK_n = 1/(1 + \exp(-(-2.75817 - 0.027635 CR_n + 3.709 DEF_n^{0.5} + 0.0488 H_n))) \quad (22)$$

where

$PTK_n$  = probability of topkill for Prognosis Model sample tree  $n$

$CR_n$  = crown ratio (percent) of tree  $n$

$H_n$  = height in feet of tree  $n$

$DEF_n$  = defoliation of tree  $n$ .

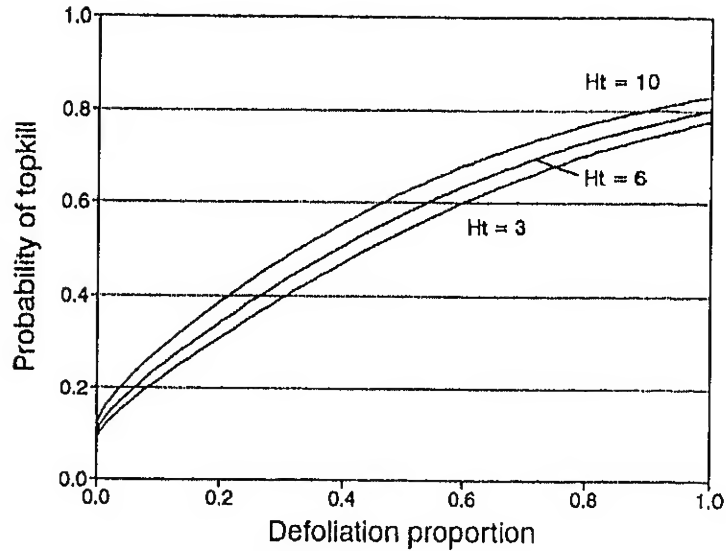


Figure 11—Probability of small-tree topkill plotted over defoliation proportion for three tree heights (modified from Ferguson 1988).

In this case,  $DEF_n$  is defined as follows. A running average proportion of new-foliage-retained biomass in the tops of trees is computed by host and tree-size class during each year of the model run ( $AVT_{hsT}$ , where  $T$  is the number of years the model has run thus far). The running average requires that the Budworm Model has run at least 3 years. The minimum value of this running average is stored. Its complement is the maximum average defoliation over the length of the Prognosis Model cycle. Ferguson's original model used average defoliation over the entire tree rather than average over just the tops of trees. The data used to fit the model were composed mostly of small trees where the defoliation is similar over all crown thirds. Because the model is applied to larger trees that experience differential defoliation between crown thirds, defoliation at the tops of trees was used in equation 22.

Formally stated,  $AVT_{h1T}$  is 1.0 for  $T = 1$  and 2. For  $2 < T < 6$ ,

$$AVT_{h1T} = \sum_t PRB_{h1t} / \min(T, 5) \quad (23)$$

Only 5 years of defoliation are counted. That is, when  $T > 5$ , the summation  $\sum_t$  starts at  $T-4$ , rather than 1.

At end of the Prognosis Model cycle, the min is found and then  $DEF_n$  is computed:

$$AVTM_{h1} = \min (AVT_{h11}, AVT_{h12}, \dots, AVT_{h1T}) \text{ and} \quad (24)$$

$$DEF_n = \beta ((1 - AVTM_{h1}), 0.03) \quad (25)$$

where tree  $n$  is of host  $h$  and a small tree (size  $s = 1$ ).  $DEF_n$  is then used in equation 22 to compute  $PTK_n$ .

If  $PTK_n$  is greater than a uniform random number, the tree is actually topkilled. The amount of topkill is computed by a separate function. Ferguson (1988, p. 7) reported no success in building a function that relates the amount of topkill (he uses the term dieback) to the amount of defoliation, nor to any other predictor variables. Therefore, he characterized his data with a Weibull distribution function. His recommended model is used in the Budworm Model exactly as proposed.

Figure 12 illustrates Ferguson's function. The way this function is applied in the model is simple. A uniform random number between 0 and 1 is drawn for each sample tree. The random number is a point on the axis labeled *proportion of trees* in figure 12. The corresponding point on the axis labeled *proportion of stem killed* is found, thereby completing the computation. Formally stated, let  $u_n$  be a uniform random number on (0, 1) for tree  $n$ ; then the portion of the stem killed is

$$PRK_n = 0.05684 (-\ln u_n)^{1.7036} \quad (26)$$

**Medium and Large Trees**—Ferguson's (1988) models cover regeneration-sized trees, which were less than 7 m (23 ft) in height. For larger trees another set of models were conceived by Bruce Hostetler, Tommy Gregg, and the author in a 1988 meeting held at Hostetler and Gregg's office, Forest Pest Management, Pacific Northwest Region, Forest Service, Portland, OR. These models represent the professional judgment of Hostetler and Gregg; their equation form is a modification of the Weibull p.d.f. The probability of topkill is computed and compared to a uniform random number as done for small trees. For trees that are topkilled, the amount of topkill is computed using a separate model. Both models are functions of defoliation, computed exactly the same way as done for small trees (equations 23-25). Figure 13 illustrates the probability of topkill model:

$$PTK_n = B1(1 - \exp(-(B2(DEF_n + 1))^{B3})) \quad (27)$$

where  $B1 = 0.96$ ,  $B2 = 0.65$ , and  $B3 = 14$ , for species GF, AF, or WF;  $B1 = 0.90$ ,  $B2 = 0.60$ , and  $B3 = 11$  for DF and ES.

Figure 14 illustrates the proportion of stem killed ( $PRK_n$ ) model. The model is exactly the same as equation 27, except for species GF, AF, and WF:  $B1 = 0.0960$ ,  $B2 = 0.717$ , and  $B3 = 7.92$ ; and for species DF and ES:  $B1 = 0.2545$ ,  $B2 = 0.641$ , and  $B3 = 6.60$ .

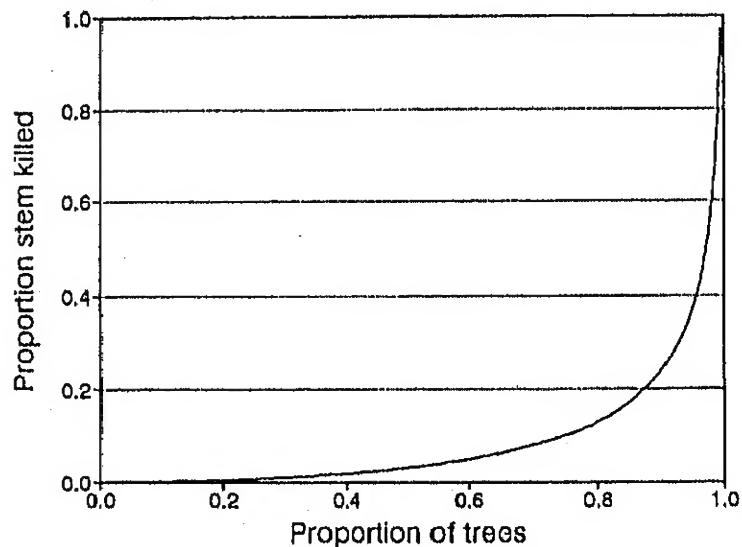


**Figure 12**—Proportion of stem killed plotted over proportion of small trees that are topkilled (from Ferguson 1988).

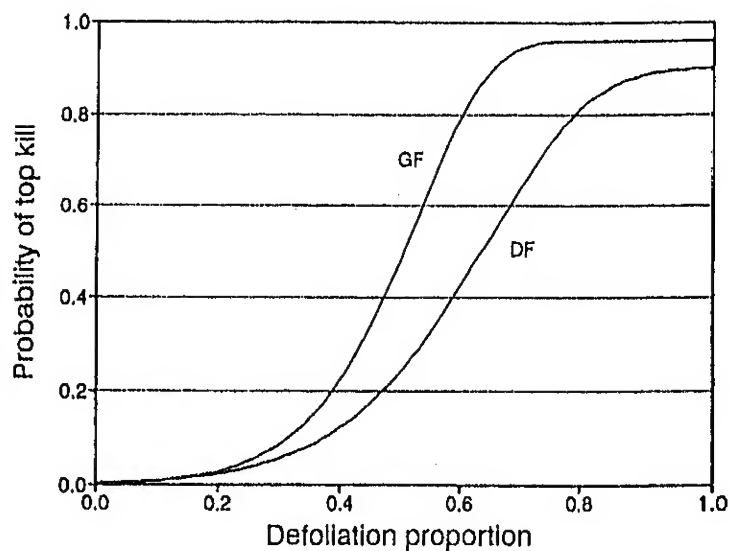


Figure 13—Probability of medium- and large-tree topkill plotted over defoliation proportion. The line conceived for GF is used for AF and WF; the line conceived for DF is used for ES.

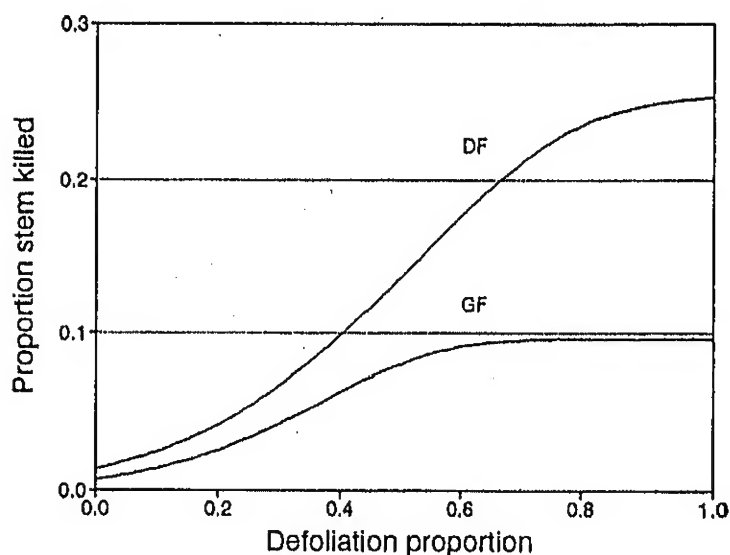


Figure 14—Proportion of medium and large tree stems killed plotted over defoliation proportion. The line conceived for GF is used for AF and WF; the line conceived for DF is used for ES.

## Height Growth

For trees that have not been topkilled, budworm-caused defoliation can result in reduced height growth. For small trees, Ferguson's (1988) height growth model was adapted to estimate the effects of defoliation. For medium and large trees, Nichols' (1988a, b) models are used.

**Small Trees**—Ferguson (1988, p. 7) published a small-tree height growth equation of the general form  $\ln HG = \sum_i B_i X_i$ , where  $B_i$  are regression coefficients and  $X_i$  are independent variables. The independent variables include two measures of defoliation:  $X_1$  is for the first 2 years of the 6-year measurement period and  $X_2$  for the most recent 4 years. Most of the regression coefficients, including  $B_1$  and  $B_2$  are species specific.

This equation can readily be adapted for use in modifying an estimate of height growth to account for defoliation. Let  $PEHG$  be the proportion of expected height growth. If normal height growth is  $HGN$ , then height growth given defoliation is  $HGD = HGN(PEHG)$ . Also,  $PEHG = HGD/HGN$  and  $\ln PEHG = \ln HGD - \ln HGN$ .

Ferguson's equation can be used to compute normal growth and height growth given defoliation. That is,  $\ln HGN = \sum_i B_i X'_i$ , where  $X'_1 = X'_2 = 0$ , and  $\ln HGD = \sum_i B_i X_i$ , where  $X_1 > 0$  and  $X_2 > 0$ . For a given tree,  $X'_i = X_i$  for  $i > 2$ . Therefore,

$$\begin{aligned} \ln PEHG &= (B_1 X_1 + B_2 X_2 + \dots + B_n X_n) - \\ &\quad (B_1 X'_1 + B_2 X'_2 + \dots + B_n X'_n) \\ &= B_1 (X_1 - 0) + B_2 (X_2 - 0) \end{aligned} \quad (28)$$

Imposing the simplifying assumption of letting  $X_1 = X_2 = X$ , we have

$$PEHG = \exp((B_1 + B_2)X) \quad (29)$$

The values for  $B_1$  and  $B_2$  are species specific. Their sums by species are as follows: for AF (also used for WF),  $-2.3661$ ; for DF,  $-2.4757$ ; for GF,  $-2.0008$ ; and for ES,  $-2.9171$ . Figure 15 illustrates the curves.

Equation 29 is used to compute the proportion of expected height growth on small trees. It is a 5-year model, which means that it is useful for modifying 5-year height growth. The defoliation measure is similar to that used in the topkill model except that the average is taken over 5-year intervals on the top third.

Let  $PEHG_{hsT}$  be the proportion of expected height growth on host  $h$ , tree size  $s$  (1 = small in this case), at time  $T$ , when  $T$  is 5 and again when  $T$  is 10. For a 5-year-long Prognosis Model cycle,

$$PEHG_{h15} = \exp(B_h (1 - AVT_{h15})) \quad (30)$$

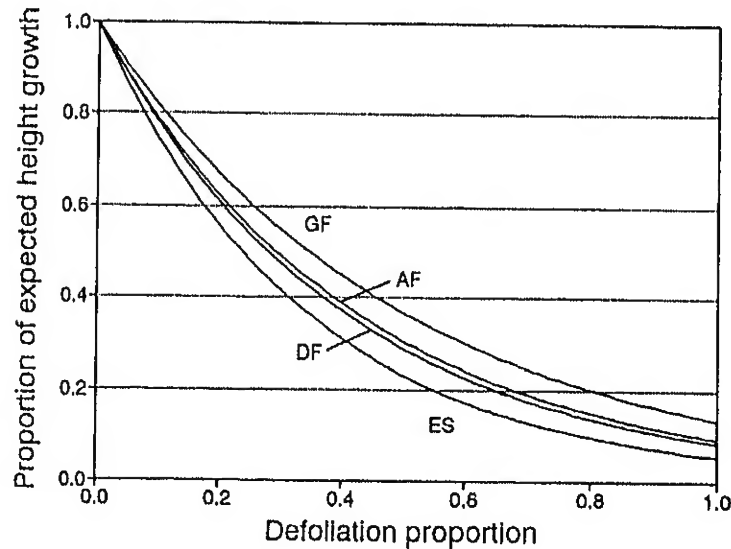


Figure 15—Proportion of small-tree expected height growth plotted over defoliation proportion (from Ferguson 1988). The line for AF is also used for WF.

where  $B_h$  are the species-specific constants described above, and  $AVT$  is computed in equation 23. If a 10-year-long cycle is used, the result of equation 30 is divided by 2, the second 5-year part of the 10-year interval is computed, divided by 2, and the sum of these two estimates is the proportion of expected 10-year height growth. If a Prognosis Model cycle length is used that is not evenly divided into 5-year-long intervals, the model is applied using as close to 5-year-long intervals as reasonably possible.

$PEHG_{hsT}$  is an average for the trees in a given class. The Budworm Modeling System assumes that the variances of  $PEHG_{hsT}$  are related to their averages like the variances of defoliation measures are related to their averages (equation 20). The available data, described in the section on using the Beta distribution, were used to verify this assumption. While the bases for making the assumption are not strong, the alternative of ignoring the variation between trees is a greater evil. Given the Prognosis Model estimate of height growth on tree  $n$  is  $HG'_n$ , then

$$HG_n = HG'_n \beta(PEHG_{hsT}, 0.03) \quad (31)$$

is the height growth on defoliated tree  $n$ , where tree  $n$  is of host  $h$  and size  $s$ .

**Medium and Large Trees**—Nichols (1988b) related growth to defoliation on large trees. His model for  $PEHG_{hst}$  is

$$PEHG_{hst} = 0.193 AVT_{hst}^{(0.3814 - 0.0212 M1)} M1^{0.5509} \quad (32)$$

where  $M1 = PEG_{hs(t-1)}$  when  $t > 1$ , and 1 otherwise. When  $s = 1$

$$AVT_{h15} = (\sum_t \sum_{c=1}^3 PRB_{hct1})/3T \quad (33)$$

for  $s = 2$ ,  $AVT_{h2T} = (\sum_t \sum_{c=4}^6 PRB_{hct1})/3T$ , and for  $s = 3$ ,  $AVT_{h3T} = (\sum_t \sum_{c=7}^9 PRB_{hct1})/3T$ . Conditions controlling the summation on  $t$  described for equation 23 also apply to equation 33.

Equation 33 is computed once for each year of the Prognosis Model cycle. Figure 16 illustrates the function's behavior for several values of  $M1$ .

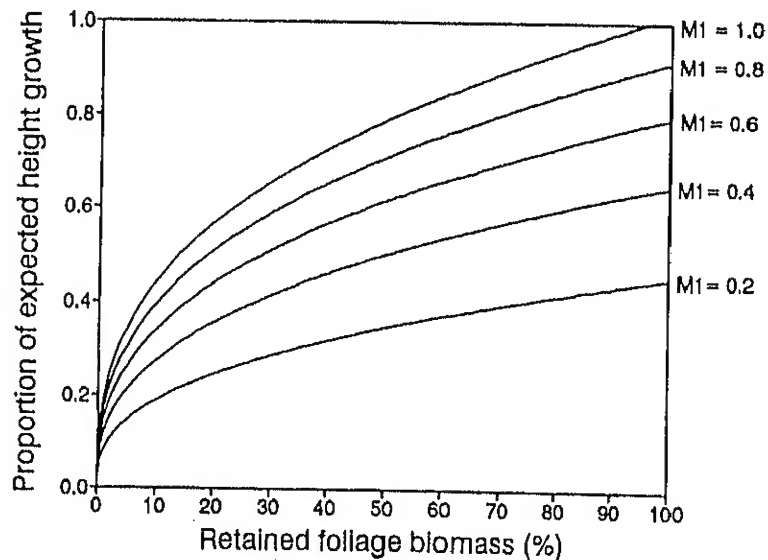


Figure 16—Proportion of medium- and large-tree expected height growth plotted over defoliation proportion (from Nichols 1988b), for various levels of  $M1$  (see equation 32).

The adjustment of the Prognosis Model growth estimate uses equation 31, that is,

$$HG_n = HG'_n \beta (\sum_t PEHG_{hst}/T, 0.03) \quad (34)$$

## Diameter Growth

Nichols' (1988b) model for proportion of expected diameter growth, which is measured in squared diameter increment,  $PEDDS_{hst}$ , has the identical form as equation 32. However, the constants are different resulting in slightly different curves (fig. 17). The equation is

$$PEDDS_{hst} = 0.084 AVT_{hst}^{(0.4725 - 0.0700 MI)} MI^{0.3241} \quad (35)$$

where  $MI = PEDDS_{hs(t-1)}$  when  $t > 1$  and 1 otherwise; and  $AVT_{hst}$  is computed using equation 33.

This equation is applied the same as the height growth equation (32). Diameter growth reductions are computed using this model for all three tree-size classes.

## Mortality

The probability of individual tree mortality in budworm-infested forests has been studied with little general success. Both Ferguson (1988) and Nichols hoped to develop functions but received insufficient cooperation from nature. The budworms did not kill many sample trees, so the sample size was too small to support proposed analyses. Alfaro and others (1982) measured plenty of mortality on one stand near Pemberton, BC. They published two models that represent their data. The first relates mortality to tree size ( $PRMD$ , equation 36, fig. 18, line A), and the second relates mortality to cumulative defoliation ( $PRMC$ , equation 37, fig. 18, line B):

$$PRMD_n = 140.75 \exp(-0.057 D_n) \quad (36)$$

$$PRMC_n = 4.17 (10^{-11}) CMD_n^{4.78} \quad (37)$$

where  $D_n$  is d.b.h. in centimeters (for  $D_n$  in inches, substitute  $-0.1448$  for  $-0.057$ ), and  $CMD_n$  is a 5-year cumulative percentage defoliation; both are for tree  $n$ .

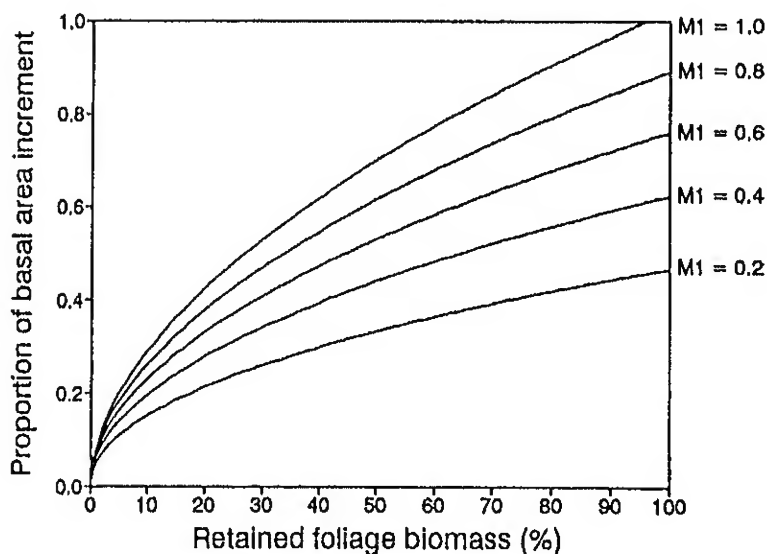
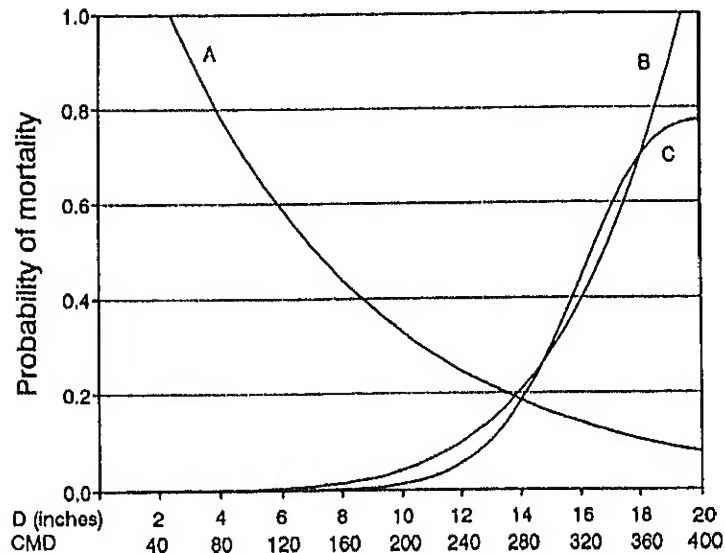


Figure 17—Proportion of expected basal area increment plotted over defoliation proportion (from Nichols 1988b), for various levels of  $MI$  (see equation 35).



**Figure 18**—Line A is probability of mortality plotted over d.b.h. ( $D$ , equation 36); and line B is probability of mortality plotted over cumulative percentage defoliation ( $CMD$ , equation 37). Lines A and B are from Alfaro and others (1982). Line C is a refit of the data represented by line B; see equation 39.

In a much more extensive study, Alfaro (1986) found that suppressed trees suffered significantly higher mortality rates than nonsuppressed trees. Slope and site quality were also related to mortality in budworm-defoliated stands. The number of years a stand suffered “severe” defoliation accounted for 47 percent of the variation in the mortality rate data. This finding is generally consistent with the model proposed from the Pemberton site, equation 37. That is, high values of  $CMD$  can only occur when there are several years of severe defoliation.

In 1985, Crookston (1985, p. 216) published a combined version of equations 36 and 37. This model has been criticized as being an unrealistic extrapolation of Alfaro and others’ (1982) work. It predicts low mortality rates for large trees even when  $CMD$  is high.

None of the models found in the literature are satisfactory for inclusion in the Budworm Modeling System. Equation 36, the function of diameter, assumes that stand structure and defoliation are the same as found at the Pemberton site. Equation 37 ignores site, competition, and tree-size effects that have been documented. Simple rates indexed by site or competition ignore the interactions with other variables.

Clearly, an extensive study of budworm-caused mortality is needed. In the absence of such a study, and in the presence of work that has been accomplished, the mortality model illustrated in figure 19 has been inserted into the Budworm Modeling System. The function used to represent the response surface is described below, after a biological interpretation is presented.

$RBAL_n$  is the relative basal area in trees larger than tree  $n$ . It is computed by dividing the amount of basal area in trees larger than tree  $n$  ( $BAL_n$ ) by the maximum basal area ( $BAMAX$ ) that typically exists for the site:

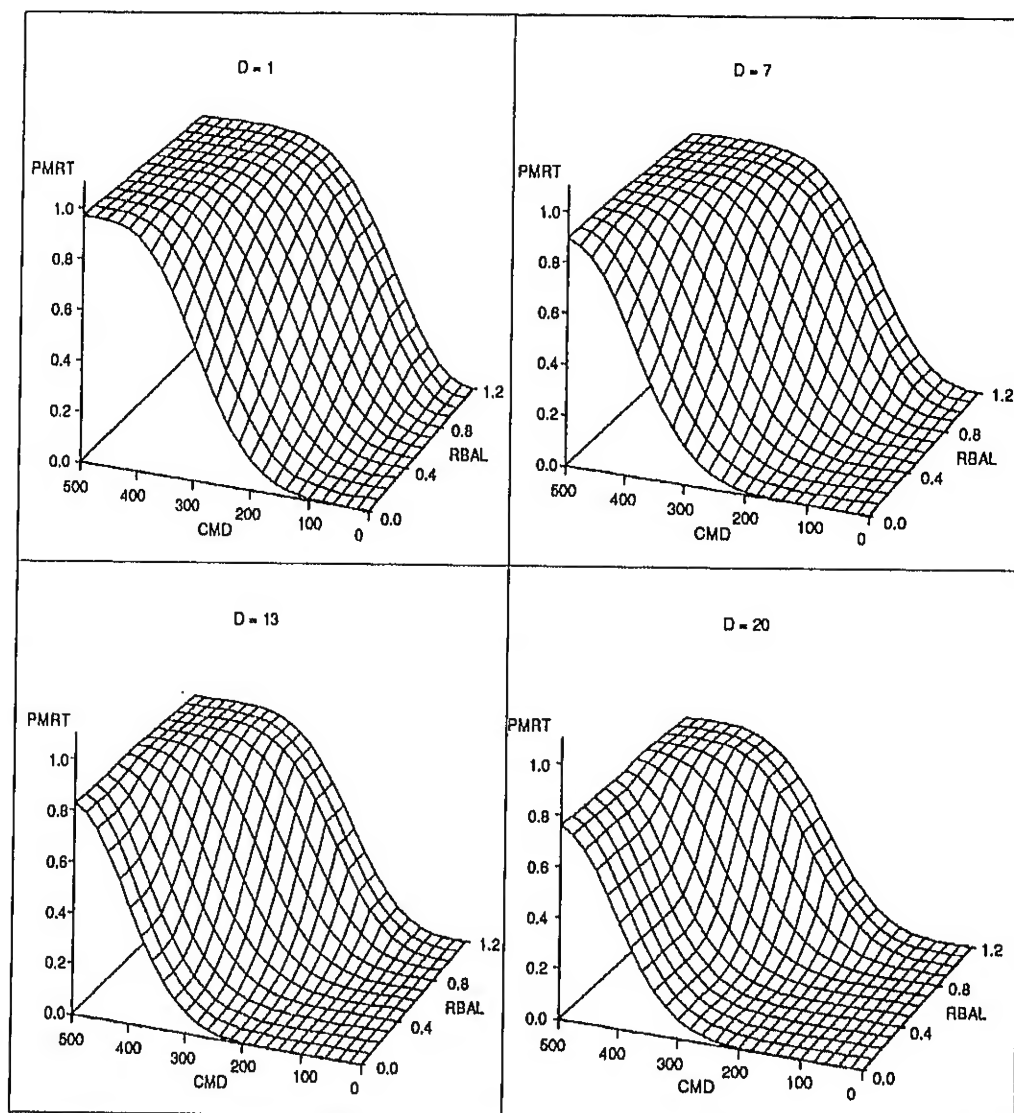


Figure 19—Probability of mortality ( $PMRT$ ) plotted over cumulative defoliation ( $CMD$ ) and relative basal area in larger trees ( $RBAL$ ) for several levels of d.b.h. ( $D$ ). See equations 39-43.

$$RBAL_n = BAL_n / BAMAX \quad (38)$$

Values of  $RBAL_n$  near zero indicate that tree  $n$  is growing with little competition. Tree  $n$  could be any size tree growing in a stand with little total basal area, or it could be the largest of many large trees. If  $RBAL_n$  is near or above 1.0, then tree  $n$  is under competition. A small tree, growing under a large overstory in a stand that is at or above  $BAMAX$ , will have a high  $RBAL_n$ . Site quality is inherent in this metric because a stand of moderate total basal area, growing on a poor site, could be close to its maximum. In the Prognosis Model,  $BAMAX$  is indexed by stand habitat type or it can be set by the model user.

Figure 19 indicates that the probability of mortality,  $PMRT_n$ , increases with increasing values of  $RBAL_n$ . Increasing values of  $CMD_n$  also increase the probability of mortality. For small trees, the mortality rate increases with increasing  $CMD_n$  and increasing  $RBAL_n$  faster than it does for large

trees. Furthermore, the maximum mortality rate for large trees growing without competition is lower than the maximum rate is for large trees growing with competition.

The equation for  $PMRT_n$  is an alteration of the Weibull p.d.f.; line C in figure 18 illustrates the shape of the function

$$PMRT_n = B1(1 - \exp(-(B2(CMD_n + 1))^{B3})) \quad (39)$$

where  $B1 = 0.78$ ,  $B2 = 0.003044$ , and  $B3 = 8.429$ . The values of  $B2$  and  $B3$  were found by fitting Alfaro and others' (1982) published data points to equation 38, after arbitrarily setting the upper asymptote,  $B1$ , to 0.78.

Equation 39 is more flexible than equation 37.  $B2$  controls at what point along the  $CMD$  axis the curve starts to climb,  $B3$  is a power term that controls how steep the climb becomes before  $B1$  flattens it off.

In the final model  $B1$  is a function of tree d.b.h. ( $D_n$ ).  $B2$  and  $B3$  were set equal to functions of  $D_n$  and  $RBAL_n$  that were crafted to provide the desired behavior.

Let  $RBAL_n = \min(RBAL'_n, 1)$ , where  $RBAL'_n$  is computed in equation 38, and let  $D_n = \min(D'_n, 20)$ , where  $D'_n$  is the actual tree d.b.h. Then

$$B1_n = 0.98 - 0.01 D_n \quad (40)$$

$$XM_n = 0.02 D_n + (0.5 + 0.03 D_n)(1 - RBAL_n) \quad (41)$$

$$B2_n = 0.00575 - 0.00645 XM_n + 0.0031 XM_n^2 \quad (42)$$

$$B3_n = 2.27 - 2.94 XM_n + 1.84 XM_n^2 \quad (43)$$

Equation 39 is modified such that  $B1$ ,  $B2$ , and  $B3$  are subscripted by tree  $n$ . The only remaining detail of the mortality model concerns how  $CMD_n$  is computed.

For each year in a Prognosis Model cycle, the overall average tree defoliation ( $CDEF_{hsT}$ ) is computed for host  $h$ , size class  $s$ , and year  $T$ . (Recall that  $T$  is the number of years the model has run. For example, in the fourth year of a run,  $T = 4$ , in the tenth year,  $T = 10$ .) This is not defoliation of just the new foliage; it represents the defoliation in general, over the entire tree. It corresponds to the defoliation measure used by Alfaro and others (1982). For  $T \geq 5$ , and  $s = 1$

$$CDEF_{hsT} = 100 \sum_{t=T-4}^T (1 - (\sum_{c=1}^3 \sum_a BAF_{hcat} / \sum_{c=1}^3 \sum_a APB_{hcat})) \quad (44)$$

where  $APB$  and  $BAF$  are defined in equations 4 and 6, respectively. When  $s = 2$ , the summation over  $c$  includes 4, 5, and 6; and when  $s = 3$ , the summation over  $c$  includes 7, 8, and 9.

The maximum value of the  $CDEF_{hst}$  is

$$CMDF_{hs} = \max(CDEF_{hs5}, CDEF_{hs6}, \dots, CDEF_{hsT}) \quad (45)$$

$CMDF_{hs}$  has a theoretical range of 0 to 500, where 500 means that a tree is completely stripped of all foliage each year of 5 consecutive years. The Beta distribution is used to generate an individual tree estimate:

$$CMD_n = 500 \beta(0.002 CMDF_{hs}, 0.03) \quad (46)$$

where tree  $n$  is of host  $h$  and size  $s$ .

Therefore, the mortality model used in the Budworm Modeling System includes elements of tree size, site quality, competition, stand size, and tree defoliation—including variation in defoliation between individual trees in a tree-size class. The model estimate is assumed to be a 10-year mortality rate and is scaled (by discounting and compounding) for different Prognosis

Model cycle lengths. The Prognosis Model estimate of background mortality is used in place of the Budworm Model estimate if the background rate is higher than the model rate.

## Damage Model Behavior

The behavior of the damage model depends both on the damage model formulations and the behavior of the foliage dynamics model. By tracking the numerator and denominator for expressions of defoliation, the foliage dynamics model provides the most important variable controlling damage. The behavior of the foliage dynamics model has been illustrated for three defoliation sequences (cases 1-3, see table 11 and fig. 3-6). Recall that case 1 portrays sustained heavy defoliation, case 2 portrays heavy defoliation that stops after 5 years, and case 3 portrays alternating light and heavy defoliation. All tree-size classes received the same initial defoliation profile in these illustrative runs, and in all cases the model was run for one 10-year-long cycle.

Illustrations of damage model behavior for these three cases follow. The Bear Gulch stand data were run for each case, and outputs from the Budworm Modeling System's STATDATA option (Crookston and others 1990, p. 56) were used to generate the graphs. The only host species in this data set is Douglas-fir, so species differences described for some of the component models are not illustrated.

**Topkill**—The top part of figure 20 is a scatter plot of the probability of topkill plotted over tree height for individual trees. The symbol for each point corresponds to the defoliation case; that is, symbol 1 is for case 1 and so on. Note that small trees are those below 23 feet (7 m), and the probability of topkill (equation 22) for them is different than for medium and large trees (equation 27). Therefore, it is not surprising to see different model behavior for trees below versus above the 23-foot threshold.

Defoliation is measured as the maximum average over 5 years (equation 24). The value of this measure is 0.95 for cases 1 and 2 and 0.65 for case 3. Given such a high average defoliation value and the shape of the Beta p.d.f. (fig. 10) when the mean approaches 0.0 or 1.0, the variation about a mean of 0.95 is quite low. That is, if the mean defoliation proportion is 0.95, most of the individuals will fall near 0.95. The shape of the probability of topkill model for Douglas-fir (fig. 13) is very flat for the range of defoliations 0.90-1.0. Therefore, the individual probabilities of topkill for cases 1 and 2 are clustered on top of each other, forming a jumbled mass, near the upper asymptote of topkill function. For case 3, the probability of topkill is spread all over the plot, reflecting the variability in defoliation proportion when the mean is 0.65.

For big trees, there is no tree-size effect on topkill probability (equation 22 versus equation 27). On small trees there is an effect that can be noticed on trees below 23 feet in height.

The bottom of figure 20 is a scatter plot of the number of feet killed over tree height for each defoliation case. As in the probability models, the amount of topkill models are different for small versus medium and large trees (equations 26 and 27). The linear effect for trees simulated under cases 1 and 2 implies that similar proportions of each tree's height are killed. The reason for this behavior is identical for the clustered behavior described for the probability of topkill model. For small trees, a distribution function is used. Therefore, no correlation between proportion killed and any other variable is represented and should not be evident.

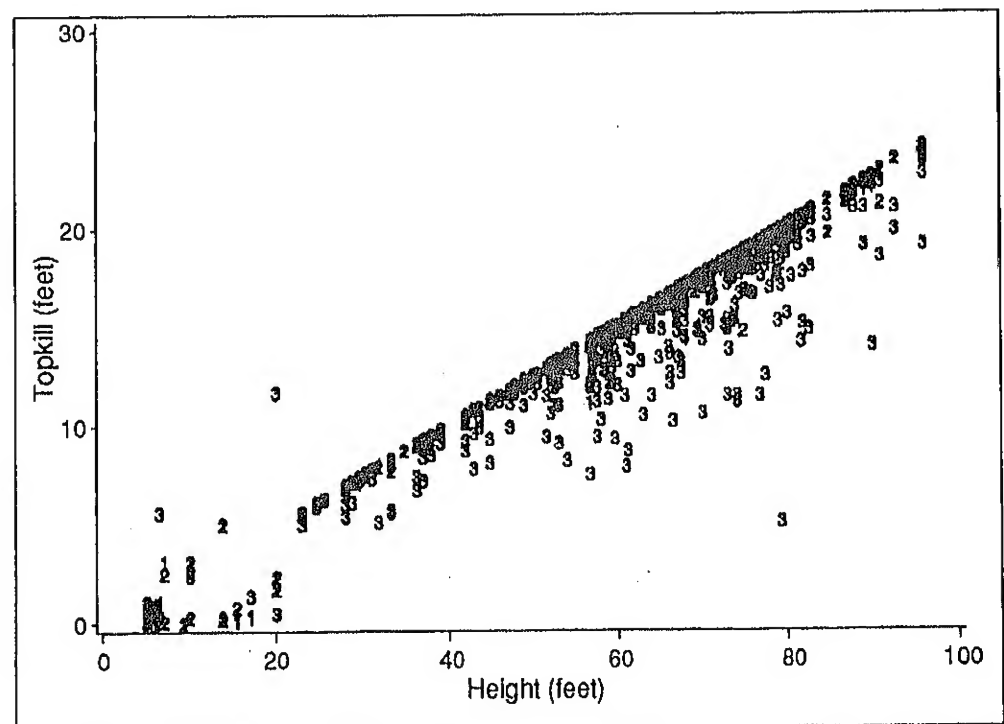
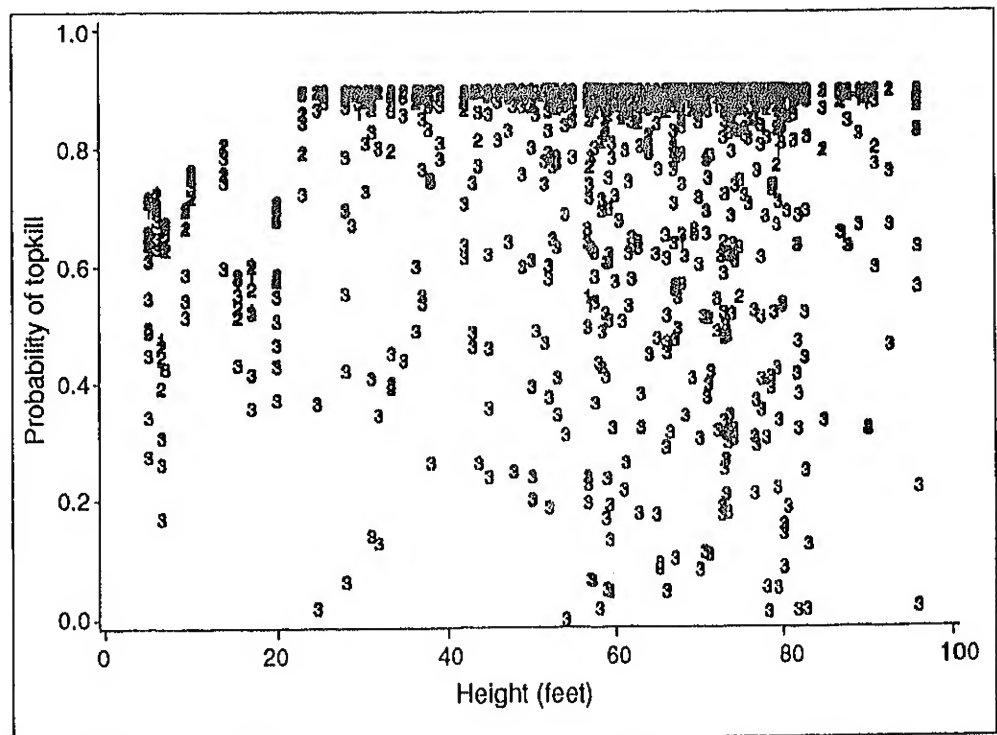


**Figure 20**—Probability of topkill (top) and amount of topkill (bottom) plotted over tree height for defoliation cases 1 through 3. There are nearly as many points for cases 1 and 2 as seen for case 3, but they plotted on top of each other forming a heaped mass.

**Proportion of Expected Growth**—Trees that are not topkilled may sustain some degree of height growth reduction; all trees may sustain diameter growth reduction. Figure 21 illustrates the proportion of expected height and diameter growth reduction for each tree-size class and defoliation case. For diameter growth, the proportion is the same for all tree-size classes. This is an expected result because the same models are used, and the defoliation profile is identical, for all tree-size classes. Case 1 hits the trees the hardest, case 2 is second hardest, and case 3 is the lightest.

The same general trend is true for proportion of height growth in medium and large trees. However, for small trees, case 2 results indicate that more of the expected height growth is retained than in case 3. This result is because (1) a different model is used for proportion of height growth in small trees (equation 29) than used for the others (equation 32), and (2) the small tree model takes the proportion in 5-year intervals. In case 2, defoliation stopped after 5 years. Equation 32 models the recovery by including a lag variable that is missing in equation 29. Therefore, the odd behavior illustrated in figure 21 is an artifact of the model and not likely a reflection of nature.

Scatter plots (fig. 22) of the proportion of expected growth plotted over tree size illustrate the effects of using the Beta distribution to represent variation between trees. As expected, there is overlap between cases, but trees run under case 1 are generally below those for case 2, and those for case 2 are below those for case 3. Note the reversal for the proportion of expected height growth on small trees: as expected, given the results displayed in figure 21, the case 3 trees are below the case 2 trees. Also note that there are fewer points plotted on the height growth plot (fig. 22, bottom) compared to the diameter growth plot (fig. 22, top). Trees that are topkilled are excluded from height growth reduction.

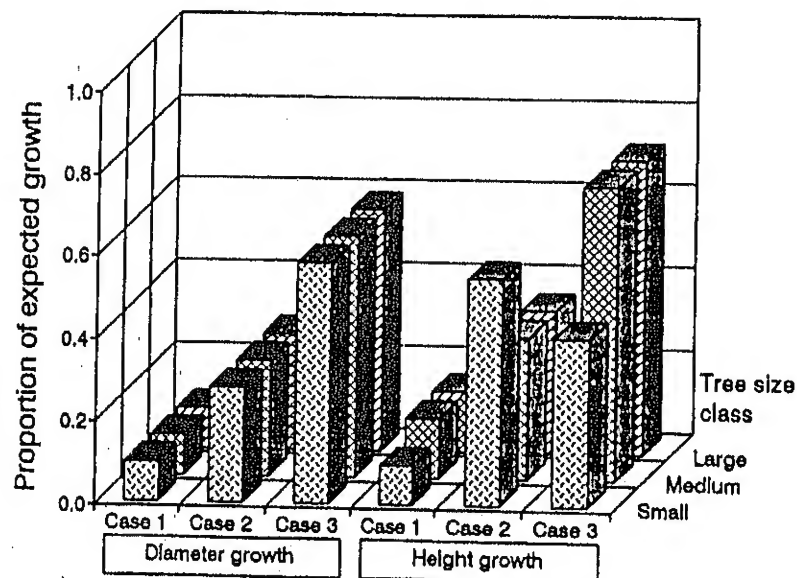
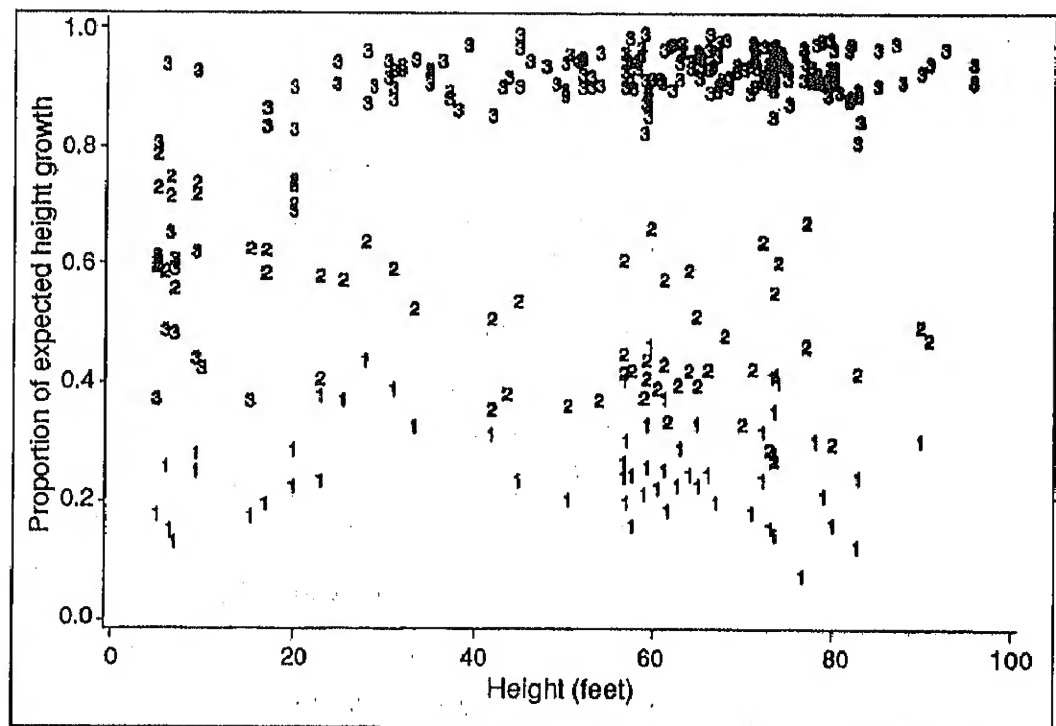
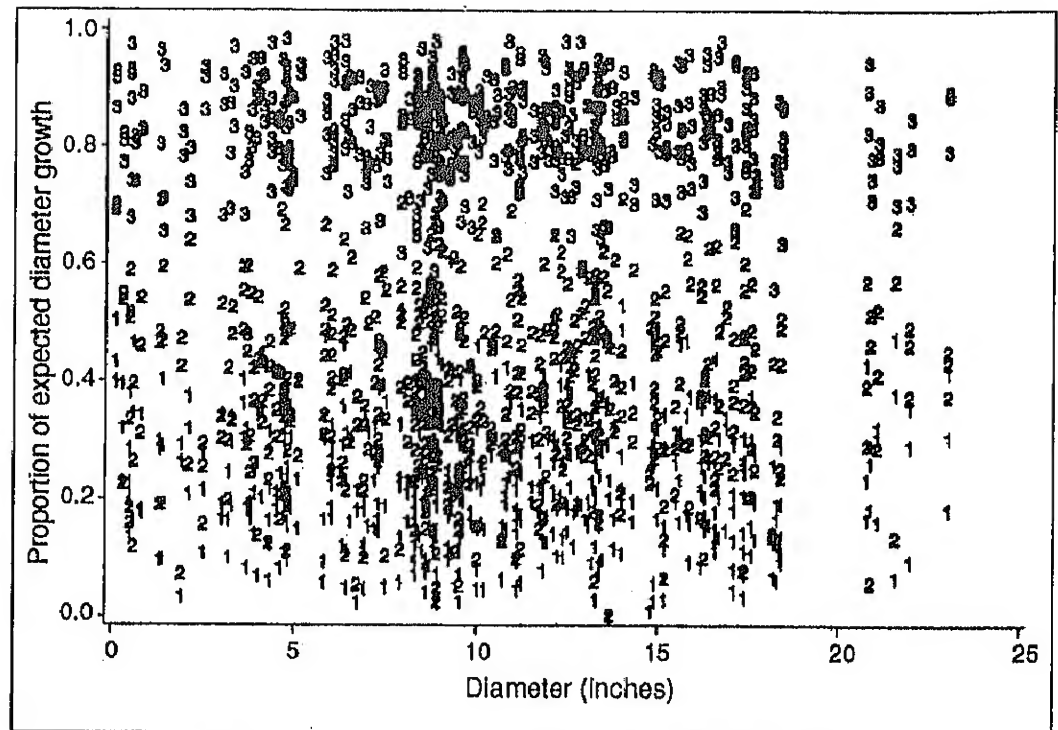


Figure 21—Proportion of expected diameter and height growth for each defoliation case by tree-size class. The odd behavior illustrated for small-tree height growth reductions is due to an equation (30) being used on small trees that differs from the equation (32) used for large trees.



**Figure 22**—Proportion of expected diameter (top) and height (bottom) growth for each Prognosis Model sample tree record by defoliation cases 1 through 3. There are many fewer trees plotted in the bottom graph because height growth reduction is relevant only on trees that were not topkilled.

**Mortality**—Mortality is chiefly a function of cumulative defoliation. The 5-year maximum *CMD* (equation 45) is charted for each tree-size class and defoliation case in figure 23. The most startling characteristics of figure 23 are the high values of *CMD* for small trees compared to medium and large trees. A higher proportion of small trees' foliage is new compared to larger trees (table 9). Therefore, when constant proportions of new foliage are removed, the overall impact of defoliation is higher on small trees than on larger trees (review equations 44-46). The ranking between cases is as expected: case 1 has the highest *CMD*, case 2 the second highest, and case 3 the lowest.

Figure 24 plots mortality rates over tree diameter for each Prognosis Model sample tree by defoliation case. The lower limits of mortality are those imposed by the Prognosis Model's own background rates. Case 1 trees generally have the highest mortality rates. The rates are highly scattered due to the effects of the Beta. Small trees die at obviously much higher rates than larger trees. This is due to the high *CMD* values for small trees and the shape of the mortality function (fig. 19) that indicates that smaller trees die at higher rates than larger trees.

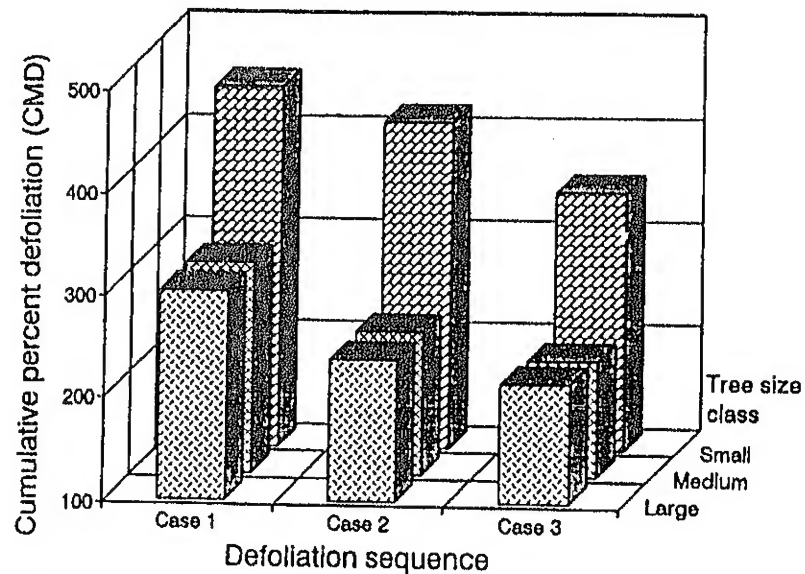


Figure 23—Cumulative percentage defoliation (*CMD*) for each defoliation case by tree-size class. Because smaller trees have a higher proportion of new foliage than large trees, values of *CMD* are higher for small trees even though percentage defoliation of new foliage is identical for all tree-size classes.

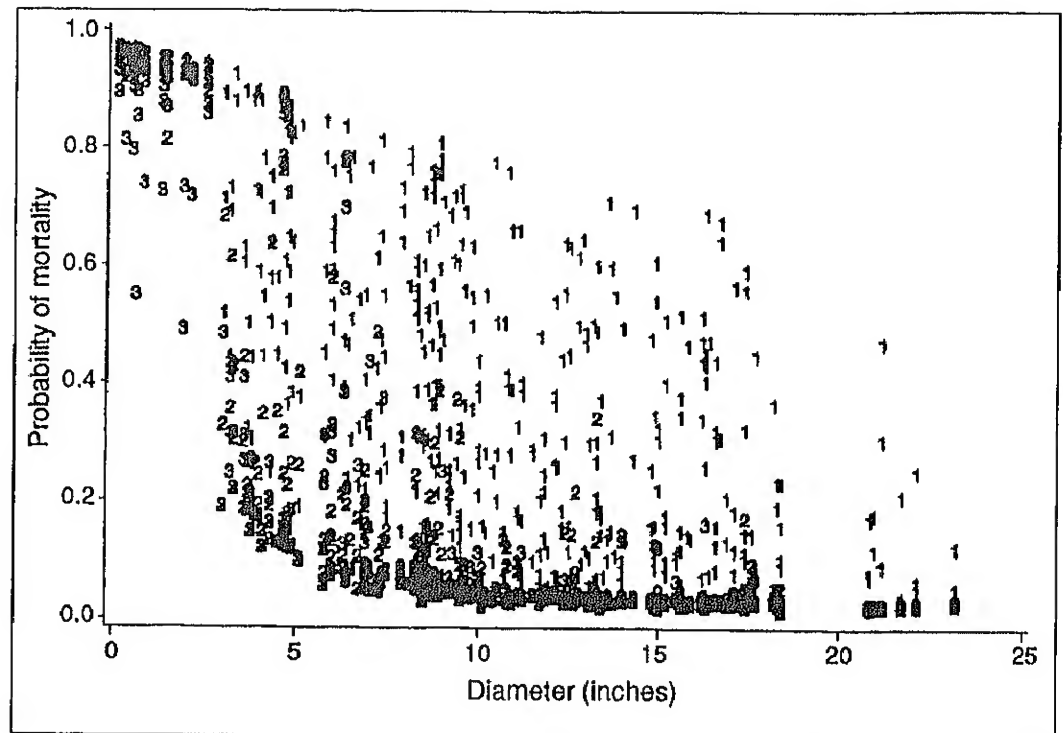


Figure 24—Probability of mortality plotted over tree diameter for each Prognosis Model sample tree record and by defoliation cases 1 through 3.

## CONCLUSIONS AND RESEARCH NEEDS

After reading the review draft of this manuscript, reviewer Michael Marsden (Rocky Mountain Station, USDA Forest Service, Fort Collins, CO) suggested being “more upbeat” in the conclusions, and offered the following:

There is a great deal of room for improvement in the foliage and damage components of the Western Budworm Modeling System. The strong points of the present components are they are logical, simple yet complete, and can be easily modified. Some of the functions in the model may seem complex but they are great simplifications of the natural system. These functions are also selected to constrain the possible results to limits natural within the system. Adjustment can be made to the model by adjusting coefficients as more information becomes available.

Marsden’s opinions about this model are as valid as mine. Much of the model is based on ideas and opinions. My original conclusions, after editing, issue a stronger call for new work and care. They follow.

The foliage and damage components of the Budworm Modeling System should be changed. The changes must result in behavior that better represents what is known about tree and budworm interactions and dynamics; otherwise the model must stand. Research is needed to support creating the new ideas, analyses, and facts required to justify model modifications.

What can this model suggest about research priorities? The foliage dynamics model is based on little data, yet I don't believe that research aimed at improving it is the highest priority. A sensitivity analysis that tests the overall model's performance relative to varying some of the relationships in the foliage dynamics model could provide convincing results to the contrary. Clearly, the assumptions relating to defoliation measurements, and therefore all the ideas surrounding the adjusted potential biomass calculations, directly impact the behavior of the damage models.

Defoliation proportion is expressed as the amount of foliage on a tree after defoliation, divided by the amount the observer expects there would have been if the tree had not been defoliated. Clearly, the divisor in this relationship is not directly observable. Yet the result, defoliation, is assumed to be field measurable without error in analyses relating defoliation to damage. Because most of the work on damage was done using some measure of defoliation, part of this model is necessarily devoted to predicting both the numerator and the denominator of defoliation relationships. These components may cause bias in the damage estimates, but I do not suspect that the qualitative behavior is wrong.

In this model, height growth, topkill, and mortality are modeled separately. During the Canada/U.S. Budworms Program, some program participants (see the acknowledgments section) suggested that mortality is simply the ultimate form of topkilling. Furthermore, topkilling simply begins with 100 percent height growth loss. Any future analyses of height growth loss, topkilling, and mortality data might profit from this idea. Including a model based on this idea in the present damage model is practical. In any case, the topkill equations should be replaced with some based on analyses whenever they are ready. Building such relationships ranks high on a research priority list.

A giant improvement over the modeling approach used here may require a totally different model. Photosynthesis creates the food for growth. Tracking photosynthetic ability with and without feeding would be a cleaner model form. What was done in this model involved attempts to track surrogate metrics of the fundamental processes. Using a physiological modeling approach would likely lead to unifying the foliage and damage components and lead to modeling topkill and tree mortality as a process.

In the meantime, it is likely that this model will be used with few modifications. A sensitivity analysis is needed both to demonstrate model behavior and component interactions and to provide guidelines to model users concerning how carefully they should measure some input data. Information regarding potential appropriate applications can be a result of sensitivity analysis. This research need ranks highest.

## REFERENCES

- Alfaro, Rene I. 1986. Mortality and top-kill in Douglas-fir following defoliation by the western spruce budworm in British Columbia. *Journal of the Entomological Society of British Columbia*. 83: 19-26.
- Alfaro, R. I.; Van Sickle, G. A.; Thomson, A. J.; Wegwitz, E. 1982. Tree mortality and radial growth losses caused by the western spruce budworm in a Douglas-fir stand in British Columbia. *Canadian Journal of Forest Research*. 12(4): 780-787.

- Beckwith, R. C.; Kemp, W. P. 1984. Shoot growth models for Douglas-fir and grand fir. *Forest Science*. 30: 743-746.
- Carolin, V. M.; Coulter, W. K. 1972. Sampling populations of western spruce budworm and predicting defoliation on Douglas-fir in eastern Oregon. Res. Pap. PNW-149. Portland, OR: U.S. Department of Agriculture, Forest Service, Pacific Northwest Forest and Range Experiment Station. 38 p.
- Cheng, R. C. H. 1978. Generating Beta variates with nonintegral shape parameters. *Communications of the ACM*. 21(4): 317-322.
- Crookston, Nicholas L.; Colbert, J. J.; Thomas, Paul W.; Sheehan, Katharine A.; Kemp, William P. 1990. User's guide to the western spruce Budworm Modeling system. Gen. Tech. Rep. INT-274. Ogden, UT: U.S. Department of Agriculture, Forest Service, Intermountain Research Station. 75 p.
- Crookston, Nicholas L. 1991. The Western Spruce Budworm Dynamics Model: version 3.1 update and notes on behavior. Gen. Tech. Rep. INT-283. Ogden, UT: U.S. Department of Agriculture, Forest Service, Intermountain Research Station. 25 p.
- Crookston, Nicholas L. 1985. Forecasting growth and yield of budworm-infested forest. Part II: Western North America and summary. In: Sanders, C. J.; Stark, R. W.; Mullins, E. J.; Murphy, J., eds. Recent advances in spruce budworms research: Proceedings, spruce budworms research symposium; 1984 September 16-20; Bangor, ME. Ottawa: Canadian Forestry Service: 214-230.
- Ferguson, Dennis E. 1988. Growth of regeneration defoliated by spruce budworm in Idaho. Res. Pap. INT-393. Ogden, UT: U.S. Department of Agriculture, Forest Service, Intermountain Research Station. 13 p.
- Hastings, N. A. J.; Peacock, J. B. 1975. *Statistical Distributions*. New York and Toronto: John Wiley and Sons. 129 p.
- Hatch, C. R.; Mika, P. G. 1978. Final report: foliage biomass estimates for Douglas-fir, grand fir, and white fir from selected DFTM outbreak areas in the western U.S. CANUSA-West final report on file at: U.S. Department of Agriculture, Forest Service, Pacific Northwest Research Station, Portland, OR.
- Jenson, E. C. 1976. The crown structure of a single codominant Douglas-fir. Seattle, WA: University of Washington. 83 p. M.S. thesis.
- Mayfield, J. E. 1984. Research note in the CANUSA Newsletter. 1984 September.
- McDonald, G. I. 1981. Differential defoliation of neighboring Douglas-fir trees by western spruce budworm. Res. Note INT-306. Ogden, UT: U.S. Department of Agriculture, Forest Service, Intermountain Forest and Range Experiment Station. 10 p.
- Moeur, M. 1981. Crown width and foliage weight of Northern Rocky Mountain conifers. Res. Pap. INT-283. Ogden, UT: U.S. Department of Agriculture, Forest Service, Intermountain Forest and Range Experiment Station. 14 p.
- Nichols, Thomas J. 1988a. Selecting foliage and growth variables for relating insect defoliation to coniferous tree growth. *Forest Science*. 34(1): 236-242.

- Nichols, Thomas J. 1988b. The relationship between western spruce budworm defoliation levels and growth of individual Douglas-fir and grand fir trees. *Forest Science*. 34(2): 496-504.
- Schmid, J. M.; Morton, M. B. 1981. Distribution of foliage on open-grown white fir and Douglas-fir in northern New Mexico, U.S.A. *Canadian Journal of Forest Research*. 11(3): 615-619.
- Sheehan, Katharine A.; Kemp, William P.; Colbert, J. J.; Crookston, Nicholas L. 1989. The Western Spruce Budworm Model: structure and content. Gen. Tech. Rep. PNW-241. Portland, OR: U.S. Department of Agriculture, Forest Service, Pacific Northwest Research Station. 70 p.
- Stage, Albert R. 1973. Prognosis Model for stand development. Res. Pap. INT-137. Ogden, UT: U.S. Department of Agriculture, Forest Service, Intermountain Forest and Range Experiment Station. 32 p.
- Thomson, A. J. 1979. Evaluation of key biological relationships of western budworm and its host trees. Res. Rep. BC-X-186. Victoria, BC: Environment Canada, Canadian Forestry Service, Pacific Forest Research Centre. 19 p.
- Wyckoff, William R.; Crookston, Nicholas L.; Stage, Albert R. 1982. User's guide to the Stand Prognosis Model. Gen. Tech. Rep. INT-133. Ogden, UT: U.S. Department of Agriculture, Forest Service, Intermountain Forest and Range Experiment Station. 112 p.

Crookston, Nicholas L. 1991. Foliage dynamics and tree damage components of the Western Spruce Budworm Modeling System. Gen. Tech. Rep. INT-282. Ogden, UT: U.S. Department of Agriculture, Forest Service, Intermountain Research Station. 40 p.

A model called the Budworm Dynamics Model has been constructed that represents the population dynamics and feeding. This model is linked to the Prognosis Model, an individual-tree, distant-independent stand growth model widely used in western North America. In this paper, a foliage dynamics model is presented that translates the tree attributes carried in the Prognosis Model into foliage biomass that serves as a substrate for budworms. A tree damage model is presented that translates budworm-caused defoliation into estimates of reduced tree growth, increased mortality, and topkilling.

KEYWORDS: simulation, *Choristoneura occidentalis* Freeman, Prognosis Model

---

---

To acquire Budworm Model programs, contact: Methods Application Group, Forest Pest Management, Forest Service, U.S. Department of Agriculture, 3825 East Mulberry Street, Fort Collins, CO 80524-8357, or Nicholas L. Crookston, Intermountain Research Station, Forest Service, U.S. Department of Agriculture, 1221 South Main Street, Moscow, ID 83843-4298.

---



Printed on recycled paper